SPACE-TIMES GENERATED BY COMPUTERS: BLACK HOLES WITH GRAVITATIONAL RADIATION*

Larry Smarr†

Center for Astrophysics and
Department of Physics
Harvard University
Cambridge, Massachusetts 02138

The next decade will see the development of a number of new types of sensitive gravitational wave antennae which will probe the universe for a variety of new relativistic sources (see Thorne[1] for an excellent review). As a parallel program, computer programs must be designed that allow theorists to predict the gravity wave signatures of these expected sources. These programs will solve the full Einstein equations of general relativity (or other proposed theories of gravity), to build space-times containing colliding black holes or collapsing nonspherical stars.

Over the years a number of approaches have been devised to investigate portions of these spacetimes. The beautiful analytic work of Hawking,[2] Carter,[2] Robinson[3] and others has led to the result that the final stationary state of collapse or collision to form a black hole is a Kerr-Newman black hole. The early stages of the complicated nonspherical magnetohydrodynamical collapse with fully relativistic equations (assuming only a slowly time-varying gravitational field) has been computer coded by Wilson.[4] The late stages of gyrations around a black hole or neutron star have been worked out extensively using linear perturbation equations off the fully relativistic background.[5]

The only piece left is the fully relativistic, highly dynamic, nonperturbative, strong field interaction region in which most of the processes of interest to gravity wave astronomy lie (i.e., here is where the gravitational field comes into its own right as the primary dynamical entity.) One would like to be able to use computers to follow this region in detail the way other classical field theories do, e.g., hydrodynamics, electrodynamics, aerodynamics, etc. Kenneth Eppley and I have written such a program for the axisymmetric vacuum Einstein equations. We, as well as others, are currently extending this to cases of matter coupling and fully four dimensional space-times (i.e., no spatial symmetry). This article will attempt to give an overview of what goes into and what comes out of such an endeavor.

Space-Time Kinematics

When no strong gravitational fields are present, physics can be described by special relativity. Here the space-time metric has no dynamical freedom but is given by the globally Poincaré-invariant Minkowski space-time. Because of the time and space translational invariance, there exist preferred time and space coordinates. If one defines a set of *Eulerian observers* as those timelike worldlines

*This work was supported in part by the National Science Foundation.
†Junior Fellow, Harvard Society of Fellows.

normal to these flat time slices, then any matter evolution (say hydrodynamics) can be uniquely described by giving the history of variables (density, pressure, velocity, etc.) along these observers. Note that these preferred inertial observers are given *a priori* and independently of any dynamics of the matter fields. The only choice left is whether to follow the matter variables along this given set of Eulerian observers, or whether to choose a different set—say Lagrangian observers whose worldlines coincide with those of the fluid particles. Regardless of whether one uses some mixed Euler-Lagrange observers or not, time slices have been fixed in advance.

General relativity introduces the complication of a dynamical gravitational field, which by Einstein's theory means a dynamical space-time. Without time translation invariance there are no preferred time slices and no a priori Eulerian observers. One must choose which set of time slices to use to build up the space-time. The time slicing can be specified in one of two ways. The geometric properties of the slices can be stated or the properties of the trajectories (Eulerian observers) normal to these slices can be described. The former approach is more familiar to relativists, with its emphasis on differential geometry. The latter viewpoint may be more accessible to astrophysicists who have had experience with hydrodynamics.

Furthermore, now that the space-time is itself unknown (that is what we are solving for), one has to build up the space-time slice by slice as a Cauchy initial data problem. This means defining the trajectories of the Eulerian observers (space-time kinematics) simultaneously with the evolution of the gravitational field along these trajectories (space-time dynamics).

The trajectories and time slices can be mathematically described as follows:[6] Given a time slice with a unit normal vector field n^μ, also equal to the 4-velocity of the corresponding Eulerian observers, one must specify how far to evolve to the next slice at each point on the slice. A scalar function $\alpha(x^i)$ on each slice determines the lapse of proper time along each n^μ. If far from the strong field region ($r \to \infty$) the time elapsed is Δt, then $\alpha(x^i)\Delta t$ is the proper time elapsed at the point x^i. Hence, the name "lapse function"[16]‡ for α. To generate the standard Minkowski space-time slicing, one starts on a surface $t = 0$ orthogonal to the time translation Killing vector and chooses $\alpha = 1$ everywhere. This moves one to the next preferred time slice $t = \Delta t$.

From the dual observer viewpoint, one has to select the *acceleration* of the Eulerian observers at each event. These observers, while at rest in the chosen time slices, are no longer inertial, nonaccelerating, observers. Since the gravitational field attempts to focus freely falling observers ($\alpha = 1$), to remain "at rest" the observers must accelerate to balance gravity. The acceleration 4-vector of the observers normal to the time slices is given by:

$$a_i = \partial_i \ln(\alpha), \qquad a^0 = 0, \tag{1}$$

so one may refer to α as the *acceleration potential.*

In sum, the fundamental complication of geometrodynamics over flat space-time hydrodynamics is that in the former theory *one must choose the Eulerian*

‡Often symbolized by N in the literature.

observers. Now the general covariance of general relativity implies that any choice is mathematically as good as any other, in a *local* region of space-time. From the space-time engineering point-of-view nothing could be more deceiving. We need to erect a *global* space-time coordinate system if we are going to study the full dynamics of strong gravitational fields. One wants the time slices to go inside any black holes present,[7] so that the horizon development can be studied, but one wants to slice far enough into the future so that radiation generated in the strong field region has time to propagate to the weak field regions far from the holes. Most choices of α fail to meet these requirements. The simplest choice, $\alpha = 1$, fails miserably as has long been known. This geodesic slicing develops coordinate singularities (the Eulerian observers focus to a caustic) in a free-fall time scale ($t \sim M$ for black holes).

Lichnerowicz gave the way out in his classic 1944 paper.[8] He pointed out that one can choose the time slicing so that no focusing of the Eulerian observers occurs. If $\theta = \nabla^{\mu} n_{\mu}$ is the volume divergence of the Eulerian observers, then we can choose the acceleration potential α at each point by demanding $\theta = \dot{\theta} = 0$. The differential equation governing the time rate of change along the Eulerian observers (Raychauduri's equation) reads:

$$\dot{\theta} = \alpha\theta^2 - \Delta\alpha + R\alpha \tag{2}$$

Where R is the Ricci scalar of the 3-metric in the time slice. The zero-convergence time slicing can thus be obtained by solving the elliptic equation

$$\Delta\alpha - R\alpha = 0 \tag{3}$$

for the acceleration potential on each slice. From the hypersurface point of view, each $\theta = 0$ time slice has maximal volume relative to nearby slices, so this slicing is often referred to as *the maximal slicing condition*. (For a recent review see Choquet-Bruhat *et al.*[9])

A very desirable feature of the maximal slicing is that it seems to avoid hitting space-time singularities. If part of the slice is inside a black hole, then α quickly drops to zero in this region. This means that the time evolution halts automatically in regions of high enough space-time curvature, while allowing the slice to move forward to normal speed ($\alpha \simeq 1$) far from this region. This behavior of α has been observed in maximal slicings of a Schwarzschild black hole,[7] the two black hole collision,[10] strong imploding gravitational waves,[11] and model star collapses.[12] There does not as yet exist a rigorous mathematical statement of how generic this strong field maximal slicing behavior is.

Assuming we have chosen our Eulerian observers by some condition on α, we still have the freedom to choose our spatial coordinates to be constant along some other set of worldlines. This freedom is mathematically expressed by choosing *the shift vector*[13]§ β^i, which gives the 3-velocity v^i of the coordinate lines, relative to the Eulerian lines, by

$$v^i = \beta^i/\alpha \tag{4}$$

§Often symbolized by N^i in the literature.

As in flat space hydrodynamics, the coordinate observers could be chosen to comove with the matter worldlines or to form a mixed Euler-Lagrange system.

In a pure gravity problem, there is a natural radiation gauge which minimizes the shear of the coordinate observer's worldlines. This minimal shear condition[14] imposes the elliptic equation on the shift vector:

$$\Delta\beta^i + \tfrac{1}{3}D^i(D_k\beta^k) + R_j{}^i\beta^j = D^i[2\alpha(K_{ij} - \tfrac{1}{3}K\gamma_{ij})] \tag{5}$$

where D_i and Δ are the covariant derivative and the Laplacian of the 3-metric γ_{ij}.

As a specific example of maximal slicing with minimal shear coordinates, consider the Kerr metric of a rotating black hole in the standard coordinates. The t = constant slices are maximal slices whose normal Eulerian observers are the so-called ZAMO observers of Bardeen: The r, θ, ϕ = constant observers corotate with the hole, requiring a nonzero shift vector which turns out to be a minimal shear shift vector. Here it is pure differential rotation shear which is minimized.

Of course, one may simply choose $\beta_i = 0$, so that the coordinate observers coincide with the Eulerian observers. This simplifies the calculation considerably at the expense of mixing inessential coordinate shearing with the physical gravitational wave shear. In any case, it should be clear that the choice of smooth nonsingular time slices, or nonsingular Eulerian observers, by the choice of α, is the fundamental requirement, and that the choice of coordinate observers (β_i) is of secondary importance.[15]

Space-Time Dynamics[6]

Let us now turn from constructing our Eulerian observers to following the gravitational field along their worldlines. Again, one has no better source than Lichnerowicz.[8] As he shows, the Cauchy evolution separates into two distinct problems: the initial value problem and the evolution of that initial data. This is very similar to electromagnetism, where Maxwell's equations break into two kinds: equations of constraint ($D \cdot E = 4\pi\rho$, $D \cdot B = 0$) and evolution equations ($\dot{B} + D \times E = 0$, $\dot{E} - D \times B = 4\pi J$).

To see this division in our present language, suppose we have chosen a certain set of mixed Euler-Lagrange observers (α, β^i) with time slices labeled by t and spatial coordinates x^i = constant along $v^\mu = \alpha n^\mu + \beta^\mu$. Then the 4-metric, in these coordinates, can be written as[16]:

$$g_{\mu\nu} = \begin{pmatrix} -\alpha^2 + \beta_m\beta_n\gamma^{mn} & \beta_i \\ \beta_j & \gamma_{ij} \end{pmatrix} \tag{6}$$

where γ_{ij} is the 3-metric in the time slices. Just as (α, β^i) are the kinematical variables of the gravitational field, γ_{ij} are the dynamical variables. The 10 Einstein equations are a set of six second-order hyperbolic equations for the evolution of the six γ_{ij}, together with a set of four elliptic equations constraining the initial data.

Just as in Newtonian mechanics, it is convenient to introduce the "velocities" as independent field variables. From a geometric viewpoint, the appropriate object

dual to the 3-metric (first fundamental form) is the extrinsic curvature (second fundamental form). If one is evolving along the Eulerian observers n^μ, this is just the proper time derivative of γ_{ij}:

$$K_{ij} \equiv -\frac{1}{2}\,\mathcal{L}_n \gamma_{ij} = -\frac{1}{2\alpha}\,\partial_t \gamma_{ij} \tag{7}$$

where $\mathcal{L}_n$ is the Lie derivative along n^μ. By moving to a mixed Euler-Lagrange system ($\beta^i \neq 0$), one picks up "convective derivatives" as well

$$-2\alpha K_{ij} = (\mathcal{L}_t - \mathcal{L}_\beta)\gamma_{ij} = \partial_t \gamma_{ij} - D_i\beta_j - D_j\beta_i \tag{8}$$

where $\mathcal{L}_t \to \partial_t$ is the geometric version of time derivative and D_i is the 3-dimensional covariant derivative. From the Eulerian observer viewpoint, the extrinsic curvature is exactly the negative of the expansion tensor $\theta_{\mu\nu}$ of the observer congruence:

$$\nabla_\mu n_\nu = \theta_{\mu\nu} - n_\mu a_\nu = \sigma_{\mu\nu} + \tfrac{1}{3}\theta\gamma_{\mu\nu} - n_\mu a_\nu \tag{9}$$

where ∇_μ is the 4-dimensional covariant derivative and θ, a_μ are as introduced in the last section. Note for a maximal slicing ($\theta = 0$), $\theta_{\mu\nu} = \sigma_{\mu\nu}$ is just the shear tensor of the Eulerian observers.

Now the constraint equations are given by Lichnerowicz[8] as:

$$\begin{aligned} H &\equiv R + K^2 - K_{ij}K^{ij} = 2\rho \\ H_i &\equiv D_i K - D_j K_i{}^j = S_i \end{aligned} \tag{10}$$

where the matter stress-energy tensor is decomposed by our Eulerian observers into spatial pieces ($S_\mu n^\mu = S_{\mu\nu} n^\mu = 0$):

$$T_{\mu\nu} = \rho n_\mu n_\nu + S_\mu n_\nu + n_\mu S_\nu + S_{\mu\nu} \tag{11}$$

The evolution equations for the gravitational field are:

$$\begin{aligned} (\mathcal{L}_t - \mathcal{L}_\beta)\gamma_{ij} &= -2\alpha K_{ij} \\ (\mathcal{L}_t - \mathcal{L}_\beta)K_{ij} &= -2\alpha K_{mi}K_j{}^m + \alpha K K_{ij} + \alpha R_{ij} - D_i D_j \alpha \\ &\quad - \alpha S_{ij} + \tfrac{1}{2}\alpha(-\rho + S_m{}^m)\gamma_{ij} \end{aligned} \tag{12}$$

These must be supplemented by matter evolution equations, such as given by Wilson.[4]

Lichnerowicz[8] shows how to convert the nonlinear constraint equation H into a quasilinear elliptic equation. This method has since been used by many authors. York and O'Murchadha have completed[17] the program by showing how one can specify the unconstrained data in a physical way (a "first guess" at γ_{ij} and K_{ij}) and then complete this data by solving four uncoupled quasilinear elliptic equations.[18,19] Eppley and I have developed computer codes to solve these equations numerically, so in practice one can now "solve" the initial data problem (i.e., give γ_{ij}, K_{ij} to solve the constraint equations) for any given physical situation.

One sees explicitly from the evolution equations that Einstein's gravitational field equations can be regarded as describing a "dynamic space-time," i.e., that the

dynamics is contained in the time history of the changing intrinsic and extrinsic geometry of a time slice. However, one can equally well regard it as a time history of the separation and shearing of our Eulerian observers who have been sent in to record the gravitational field by its influence on the observers. In either case, the kinematics of choosing the succesive time slices, or the acceleration of the observers, is clearly separated from the dynamics by use of $(\alpha, \beta_i, \gamma_{ij}, K_{ij})$.

The only remaining task is to evolve numerically the initial data by Equation 12. This was suggested by Lichnerowicz[8] in 1944 and reinterated by DeWitt and Misner[20] in 1957. The following sections detail the implementation of that program. Before giving the numerical techniques used it is useful to recast the evolution equations as a fully first order set of quasilinear hyperbolic equations. This can be achieved by introducing the auxiliary variables:

$$D_{ijk} \equiv \partial_k \gamma_{ij} \tag{13}$$

This allows us to rewrite the evolution equations in the form[21]:

$$\partial_t \Gamma + A^i \partial_i \Gamma + F(\Gamma) = 0 \tag{14}$$

where $\Gamma = (\gamma_{ij}, K_{ij}, D_{ijk})$ is a vector with in general $(6, 6, 18) = 30$ independent components of (t, x^i). The three matrices A^i have components which depend on $(\alpha, \beta^i, \gamma_{ij})$ but not on derivatives (K_{ij}, D_{ijk}), and F is a vector whose components contain the nonlinear terms in (K_{ij}, D_{ijk}). Because this form is so similar to ordinary hydrodynamics or to a wave equation, it is very useful for numerical work; in fact, it was essential in order for us to be able to develop a stable numerical scheme.

Numerical Methods

The Einstein equations can be solved by the method of finite differences.[22] That is, one converts the space-time continuum to a space-time lattice and the differential Einstein equations to a set of differenced evolution equations. The spatial grid merely labels the observer's worldlines and so can be thought of as lattice labeled by (i, j, k). The metric functions $(\alpha, \beta^i, \gamma_{ij}, K_{ij}, D_{ijk})$ have specific values at each lattice point and vary as a function of time. In this manner the grid is fixed and does not evolve with time. The time development of the metric functions tells how physical distances and time intervals between grid points change. This is in keeping with our notion that the Eulerian observers are keeping track of components of the gravitational field while they sit at rest in their time slices.

For the remainder of the discussion, I will specialize to axisymmetric spacetimes so that all metric functions depend on only two space variables (say z and ρ) and time. The generalization to three space dimensions is straightforward. Let the rectangular background lattice spatial variables be η and ξ with even spacing $\Delta\eta$ and $\Delta\xi$. It generally is the case that one wishes the (z, ρ) coordinates to have variable spacing. For instance, one may wish a stretching of the (z, ρ) coordinates as one moves away from the strong field region. Then, one has a map $z = z(\eta, \xi)$ and $\rho = \rho(\eta, \xi)$ to define the physical grid. When differencing a field quantity, say $A(\eta, \xi)$, to represent derivatives, one uses the chain rule:

$$\partial_z A = (\partial\eta/\partial z)\partial_\eta A + (\partial\xi/\partial z)\partial_\xi A \tag{15}$$

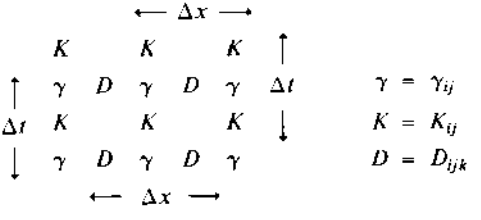
where the Jacobian coefficients $\partial_z \eta$, etc. are stored at each spatial lattice point and are independent of time. This has the advantage that the differencing ($\partial_\eta A$ etc.) occurs on a uniformly spaced grid, while leaving the flexibility to stretch (z, ρ) or match physical coordinates to boundaries.

Typically, one has to solve elliptic equations (for α, β^i) on each time slice and then advance the field quantities (γ_{ij}, K_{ij}, D_{ijk}) by hyperbolic equations. The elliptic equations are covariant and therefore have all derivatives present with coefficients functions of (z, ρ):

$$\Delta\alpha \equiv \gamma^{ij}(\partial_i\partial_j\alpha - \Gamma_{ij}{}^k\partial_k\alpha) \tag{16}$$

where $\Gamma_{ij}{}^k$ is the Christoffel symbol constructed from γ_{ij}. Eppley[10] and I have successfully solved this using standard techniques[23] such as Simultaneous Over-Relaxation (SOR). The value of $\alpha(x^i)$ at time t is used as a first guess for $\alpha(x^i)$ at time $t + \Delta t$. The only problem we encountered is that simply solving Equation 3 on each time step *does not* guarantee that the divergence $\theta = -K_{ij}\gamma^{ij}$ remains zero. Eppley‖ has devised several schemes that keep θ small by adding extra terms to Equation 3.

Usually when one has hyperbolic equations, one is very concerned numerically[23] about the formation of shock waves or very steep gradients in the field quantities. For this reason, many numerical methods contain *artificial viscosity* which spreads this steepness over several grid points. Because our earlier methods encountered numerical instabilities, Eppley and I experimented last summer at Lawrence Livermore Laboratories (LLL) with various differencing schemes. We found that a simple generalization of Lax's method[23] gave us a stable differencing scheme for the hyperbolic system.[12] This is the method we used to evolve the two-black-hole collision. Unfortunately, any method involving artificial viscosity adds dissipation to the system. As will be seen later this dissipation severely damps outgoing gravitational radiation. Following conversations with Chin, Leblanc, and Wilson[24] at Livermore, we turned to the classic staggered-mesh method. The point is that we see no tendency for steep gradients to form in the vacuum space-times we have looked at, so there seems to be no need to introduce artificial viscosity. In the staggered scheme one centers γ_{ij}, K_{ij} and D_{ijk} in space and time so as to preserve second-order accuracy:



‖C. W. Misner, Isenberg, J., and Eppley, K. R. are working on new methods of formulating "Computational Einstein equations."

That is, there are three interwoven space-time lattices, one for γ_{ij}, and one each for the first space and time derivatives: K_{ij} and D_{ijk}. This method has no artificial viscosity and thus does not dissipate the gravity waves. We used this on the evolution of pure gravitational radiation with beautiful results (see below). It is now being implemented on the two black hole code.

It should be recognized that solving systems of *partial* differential equations in two or three space variables requires much more "black magic" than solving one dimensional problems.[23] There is no unique or preferred difference representation of a differential equation. Because of storage and time limitations on even the largest computers, one in practice can never take a grid fine enough so that the solution to these various differenced versions of the same differential equation converge (see for instance Emery[25]). Each differenced equation has its own accuracy, dissipation, and dispersion which mix with the inherent dissipation and dispersion (e.g., red shift) in the Einstein equations. There are ratios such as $\Delta x/M$ or $\Delta x/\lambda$, where λ is the wavelength of the radiation, which are of order unity on coarse grids. This means higher frequency parts of the actual solution are suppressed. Thus, one must be extremely cautious about believing the result of any such numerical simulation without first having performed many consistency checks and physical arguments about what the solution "should" look like.

A great help in all this is the use of graphic displays. Whenever possible, I have tried to present functions of lattice points as two-dimensional surfaces seen in perspective. That is, consider $A(\eta, \xi)$ to be a surface whose vertical value at point (η, ξ) is given by $A(\eta, \xi)$. This surface can then be "viewed" at any angle with the (η, ξ) grid superimposed on it. Alternatively a contour map of the function may be presented. Movies of these functions were generated using Jeff Rowe's computer program DISPLAY at Lawrence Livermore Laboratories.

Gravitational Radiation

Assume that one uses the method described above to construct a space-time lattice with $(\alpha, \beta^i, \gamma_{ij}, K_{ij}, D_{ijk})$ at each point. How does one then determine the gravitational radiation which escapes from the strong field region? At present there is no rigorous method known which is practical for computer use. I will briefly describe several methods Eppley and I have used as first attempts to solve this problem.

The vacuum four-dimensional Riemann tensor $R_{\alpha\beta\gamma\delta}$ can be decomposed relative to our Eulerian observers into "electric" and "magnetic" type components[26]:

$$\begin{aligned} E_{\alpha\beta} &\equiv n^\gamma R_{\gamma\alpha\beta\delta} n^\delta \\ B_{\alpha\beta} &\equiv \tfrac{1}{2}\epsilon_\alpha{}^{\gamma\mu} n^\epsilon \gamma_\beta{}^\nu R_{\epsilon\nu\gamma\mu} \\ E_{\alpha\beta} n^\beta &= B_{\alpha\beta} n^\beta = 0 \end{aligned} \tag{17}$$

where $\epsilon_\alpha{}^{\gamma\mu} = \epsilon^{\gamma\mu}{}_{\alpha\beta} n^\beta$ and $\gamma_\beta{}^\nu = g_\beta{}^\nu + n^\nu n_\beta$. These "physical components" can then be used to build up other quantities of interest.[6] The four space-time invariants, for instance, are given by:

$$I \equiv \tfrac{1}{2}[R_{\alpha\beta\gamma\delta}R^{\alpha\beta\gamma\delta} + iR^*_{\alpha\beta\gamma\delta}R^{\alpha\beta\gamma\delta}] = 4\,W_{\alpha\beta}\,W^{\alpha\beta}$$

$$J \equiv \tfrac{1}{2}[R_{\alpha\beta\gamma\delta} + iR^*_{\alpha\beta\gamma\delta}]R^{\gamma\delta\epsilon\nu}R_{\epsilon\nu}{}^{\alpha\beta} = 8\,W_{\alpha\beta}\,W_{\gamma}{}^{\beta}\,W^{\gamma\alpha} \tag{18}$$

where $W_{\alpha\beta} = E_{\alpha\beta} + iB_{\alpha\beta}$. Computationally, $E_{\alpha\beta}$ and $B_{\alpha\beta}$ are useful because they can be built locally (at each lattice point) out of our dynamical variables[6]:

$$E^{ij} = -R^{ij} - KK^{ij} + K_m{}^i K_j{}^m$$

$$B^{ij} = D^m K^{n(i}\epsilon_{mn}{}^{j)}$$

$$E^{0\beta} = B^{0\beta} = 0 \tag{19}$$

where R^{ij} is the 3-dimensional Ricci tensor built out of γ_{ij} and D_{ijk}.

Since along an outgoing null hypersurface the Riemann tensor of a gravitational wave falls off as r^{-1}, one might expect to "see" waves by looking on spacelike hypersurfaces at the function $r^2 I$ at large distances from the source. This indeed happens as I show below. To get a more detailed picture of the radiation field one would like a local "Poynting vector" for this radiation. The above split immediately suggests the spatial vector[27] ($n \cdot P = 0$):

$$P^{\gamma} \equiv E_{\alpha\beta}\epsilon^{\beta\gamma\delta}B_{\delta}{}^{\alpha} \tag{20}$$

as an analog with electrodynamics ($\mathbf{E} \times \mathbf{B}$). This is in fact just a particular projected piece of the Bel-Robinson tensor:

$$T_{\alpha\gamma\beta\delta} = \tfrac{1}{2}[R_{\alpha\epsilon\beta\nu}R_{\gamma}{}^{\epsilon}{}_{\delta}{}^{\nu} + {}^*R_{\alpha\epsilon\beta\nu}{}^*R_{\gamma}{}^{\epsilon}{}_{\delta}{}^{\nu}] \tag{21}$$

namely

$$P^{\mu} = \gamma^{\mu\alpha}T_{\alpha\beta\gamma\delta}n^{\beta}n^{\gamma}n^{\delta} \tag{22}$$

Because this vector has units of (length)^2 times physical momentum flux, it obviously is not a local physical momentum vector for gravitational radiation and therefore does not contradict the view that gravitational energy-momentum is nonlocalizable.[28] Nonetheless, as will be shown below, it is very useful for "finding" gravitational radiation in our space-time lattice.

Once "found," we want to measure the mass-energy being carried by the radiation, as well as its angular distribution and Fourier decomposition. This is much more difficult since even the theoretical tools to use have not been sorted out. Presumably one could computerize Isaacson's prescription[29] for splitting radiation off the time changing background field and then Brill-Hartle average this radiation over several wavelengths. Such a method has not yet been devised for the computer.

Alternatively, if one has future null infinity ($\mathscr{I}^+$) conformally mapped onto the space-time lattice, then one could use the Bondi mass-loss formula[30]:

$$\frac{dM}{du} = \frac{1}{4\pi}\oint \eta\bar{\eta}\,d\Omega \tag{23}$$

Here the mass-loss is obtained by integrating over angles ($d\Omega$) on a 2-sphere of constant Bondi retarded time u at $\mathscr{I}^+$. The integrand is the modulus squared of the "news function" η, i.e., the u derivative of the asymptotic shear of the 2-sphere.

As a first step, Eppley and I have used a modified version of the Bondi mass-loss idea.# Consider a timelike hypercylinder $r = r_0$ = constant surrounding the strong field region (see FIGURE 1). Let m^α, $\bar{m}^\alpha$ be two complex null vectors spanning the 2-sphere cross sections S formed from the intersection of this hypercylinder with the t = constant slices normal to our Eulerian observers (n^α). If r_α is a form such that $r_\alpha n^\alpha = r_\alpha m^\alpha = r_\alpha \bar{m}^\alpha = 0$, then the outgoing null vector field to these 2-spheres is $\ell_\alpha = n_\alpha + r_\alpha$ and the shear σ of these 2-spheres is defined as

$$\sigma = m^\alpha m^\beta \nabla_\alpha \ell_\beta \tag{24}$$

We define our "news-function" as $\eta = -ir^2 \partial\sigma/\partial t$ at fixed $r = r_0$ and the mass-loss as in Equation 23 except $d\Omega$ is replaced by dS, the proper surface element of

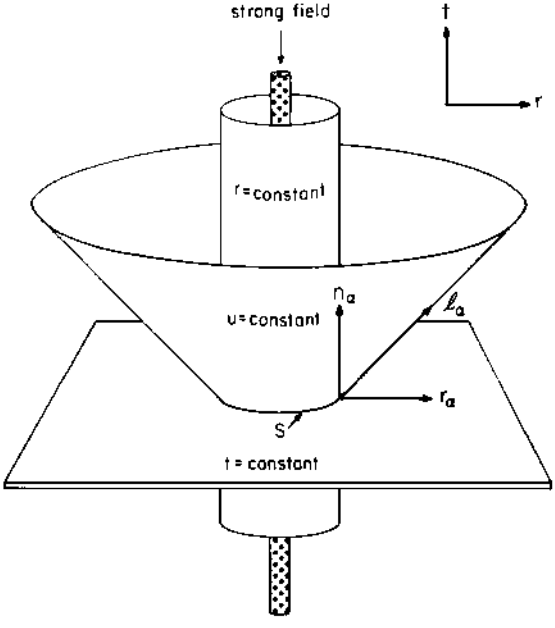


FIGURE 1. In a dynamic space-time, gravitational radiation is generated near the bounded strong field region and propagates out along a null cone (u = constant). A time slice (t = constant) intersects this cone on a 2-sphere S. This 2-sphere can also be considered as the intersection of the t = constant slice with an r = constant ℓ hypercylinder. The normal vectors to these surfaces are shown as ℓ_α, n_α, r_α with $\ell_\alpha = n_\alpha + r_\alpha$.

our 2-spheres. Specifically, the space-time line element is:

$$ds^2 = -\alpha^2 dt^2 + \gamma_{rr} dr^2 + 2\gamma_{r\theta} dr d\theta + \gamma_{\theta\theta} d\theta^2 + \gamma_{\phi\phi} d\phi^2 \tag{25}$$

so our null vectors are chosen as:

$$\ell_\beta = (-\alpha, (\gamma^{rr})^{-1/2}, 0, 0)$$

$$m^\beta = \frac{1}{\sqrt{2}} (0, 0, \gamma_{\theta\theta}{}^{-1/2}, i\gamma_{\phi\phi}{}^{-1/2}) \tag{26}$$

and our calculation of σ yields:

#The following discussion was worked out in collaboration with Paul Sommers.

$$\sigma = -\tfrac{1}{2}\{\gamma_{\theta\theta}{}^{-1}[K_{\theta\theta} + \Gamma_{\theta\theta}{}^{r}(\gamma^{rr})^{-1/2}] - \gamma_{\phi\phi}{}^{-1}[K_{\phi\phi} + \Gamma_{\phi\phi}{}^{r}(\gamma^{rr})^{-1/2}]\} \tag{27}$$

By numerically keeping track of σ at $r = r_0$, we obtain a history of the radiation pattern $dM/d\Omega\, dt$. While it is not theoretically justified that this procedure will measure the mass-loss, as a first attempt it seems reasonable. Currently research is underway to relate it rigorously to the true Bondi mass-loss at $\mathscr{I}^+$.

An immediate question is what relation this energy flux has with the covariant flux of the Bel-Robinson vector $\oint P \cdot dS$ through the same 2-sphere. I can only answer this for the case of monochromatic waves ($\sim e^{i\omega t}$) in Minkowski space-time linearized theory. There one finds the energy flux to be[31]:

$$dM/dt = \lim_{r\to\infty} \frac{r^2}{4\pi\omega^2} \oint |\psi_4|^2 d\Omega \tag{28}$$

where ψ_4 is the Newman-Penrose complex component of the Weyl tensor ($C_{\mu\nu\alpha\beta}$) which becomes asymptotically[32]:

$$\psi_4 \to \frac{\ddot{\eta}}{r} \to \frac{i\omega\eta}{r} \to -(C_{\hat{i}\hat{\theta}\hat{i}\hat{\theta}} - iC_{\hat{i}\hat{\theta}\hat{i}\hat{\phi}}) \tag{29}$$

The carets $(\hat{t}, \hat{\theta}, \hat{\phi})$ refer to an orthonormal tetrad ($\hat{\theta} = r d\theta$, $\hat{\phi} = r \sin\theta d\phi$, $\hat{t} = dt$). From the spinor form of the Bel-Robinson tenor[33] one finds that asymptotically

$$P^{\alpha} r_{\alpha} \to 2|\psi_4|^2 \tag{30}$$

So finally we have the asymptotic ($r \to \infty$) relations:

$$\dot{M} = \frac{1}{4\pi} \oint |\eta|^2 d\Omega = -\frac{1}{8\pi\omega^2} \oint P \cdot dS \tag{31}$$

(We note in passing that for an axisymmetric nonrotating space-time, both η and ψ_4 are real.) These expressions will be used below to estimate the mass-loss in our space-time lattices.

Brill Waves—A Pure Radiation Space-Time

In order to test out the methods outlined above, Eppley and I have constructed space-times containing only gravitational radiation. Unlike exact plane wave solutions, these space-times have finite energy and describe the time evolution of a "cloud" of gravitational radiation. The initial data for such space-times, assuming axisymmetry, were described by Brill[34] in 1959 and discussed extensively by Wheeler[13] in 1963. Since Brill demanded that the initial data lie on a hypersurface of time symmetry ($K_{ij} = 0$), the past of this surface is the time reverse of the future.

The character of the future evolution depends on the initial "density" of the cloud. For very weak waves, the cloud disperses to null infinity, presumably**

**Stanley Deser (private communication) stresses that there is no analytic proof that this will happen.

leaving flat space behind it. But for a cloud of waves strong enough, the nonlinearity of Einstein's equations can lead to self-coupling and formation of a black hole. The details of the evolution depends on the initial wave packet selected. These two properties are codified in the initial 3-metric by the wave profile q and wave amplitude A.

$$ds^2 = \psi^4[e^{2q}(d\rho^2 + dz^2) + \rho^2 d\phi^2] \tag{32}$$

where $q(z, \rho)$ is chosen at will. Then ψ, the conformal factor, is solved for numerically from the equation

$$\Delta\psi + \Phi\psi = 0$$

$$\Phi = \tfrac{1}{4}(q_{,\rho\rho} + q_{,zz}) \tag{33}$$

with Δ being the flat space Laplacian in cylindrical coordinates. In a numerical study of Brill's initial data, Eppley[11] picked the simplest q subject to the necessary symmetries and fall-off criteria:

$$q = \rho^2(1 + r^n)^{-1}, \qquad n \geq 4 \tag{34}$$

He and I then evolved many space-time for different values of A.

Most of our results are for $A = 10^{-3}$. For such a weak wave, one should be able to use the Einstein equations linearized off of flat space. Perhaps a clever choice of q would even lead to an analytic solution of the linearized problem. (S. Teukolsky -- private communication -- has made recent progress on a pure quadrupole Brill wave). We used our full code with the nonlinearities in to test the whole system. Because the wave is axisymmetric as well as reflection symmetric across the equator, we have only to evolve one quadrant of the (z, ρ) plane. Typically, we "stretched" the z and ρ coordinates so that $(\Delta z, \Delta\rho)$ is smaller near the center and coarser further away. The results shown below are for a spatial (z, ρ) lattice 40 × 40 (1600 points), with 120 time levels calculated into the future of the initial slice. The runs were made at Lawrence Livermore Laboratories on their CDC 7600. Computation time was about 1 millisec/zone-cycle or about 15 minutes for the full space-time.

First, we investigated the space-time curvature scalars I and J built from the Rieman tensor (Equation 18). Since the space-time is axisymmetric with no rotation, both I and J are purely real. We plot $r^2 I$ as a function (a 2-surface) over the (z, ρ) grid at each time step. This generates a movie of the time development of the function. FIGURE 2 shows $r^2 I$ at the initial moment. Note the peak would be much higher at the origin except for the factor of r^2. As one moves to the future this peak drops very rapidly, and the wave packet becomes a series of outgoing pulses. FIGURE 3 shows $r^2 I$ at $t = 5.40$. One can clearly see a precursor followed by several larger peaks. Note that the peaks are highest on the equator and fall off rapidly as one moves toward the z-axis (see the contour plot FIGURE 4), just as one would expect for quadrupole radiation. The pictures for J look similar.

To compare with this, one can plot the Bel-Robinson vector. On a time slice, this vector field can be plotted in the obvious way: the magnitude of the vector is proportional to $(P_i P^i)^{1/2}$ and the direction is that of $\mathbf{P}$. At $t = 0$ this vector is zero since B_{ij} is zero initially from Equation 19. At $t = 5.40$ (FIGURE 5) we see the Bel-Robinson vector has the same structure as the scalar invariant I.

Finally on a 2-sphere $r_0 = 3.6$, we measured our modified Bondi mass-loss (Equation 27). The radiation pattern on the 2-sphere $dM/d\Omega dt$ is shown at two times ($t = 4.80$ and $t = 5.10$) in FIGURES 6 and 7. I have scaled the overall size of the pattern by the logarithm of the integrated power, dM/dt, at that instant. One sees that at maximum power the signal is mainly quadrupolar, but at nodes of that piece, higher multipoles ("spikes") show up. The graph of the instantaneous mass loss is shown in FIGURE 8. It is surprising over how many orders of magni-

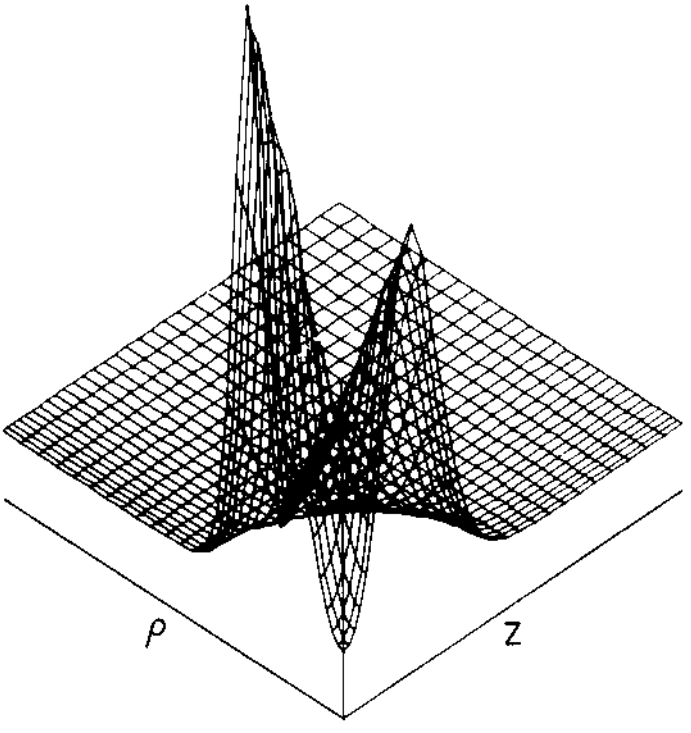


FIGURE 2. A plot of the quadratic Riemann invariant $I(z, \rho)$ times $r^2 = \rho^2 + z^2$ at $t = 0$ for the Brill gravitational wave initial data. The z-axis is to the right, and the ρ-axis is to the left. The vertical distance represents the functional value $r^2 I$ at the grid point (z, ρ). Note the initial "cloud" of radiation is concentrated near the origin and shows no wave-like characteristics. The stretched grid plotted is the actual grid used in the computer evolution.

tude our crude use of the Bondi mass-loss formula seems to give smooth answers. One sees clearly the precursor, the main pulses, and finally an exponentially decaying tail. We are not sure that the tail is real since there is no "storage ring" for Press-Goebel[35,36] black hole ringing in near-flat space. Either this tail represents radiation which at $t = 0$ was *incoming* far from $z = 0$ and then bounced off the symmetry axis at later times to become outgoing, or it is the sort of thing which the Isaacson-Brill-Hartle[29] method averages to zero. The total mass-loss through $r =$

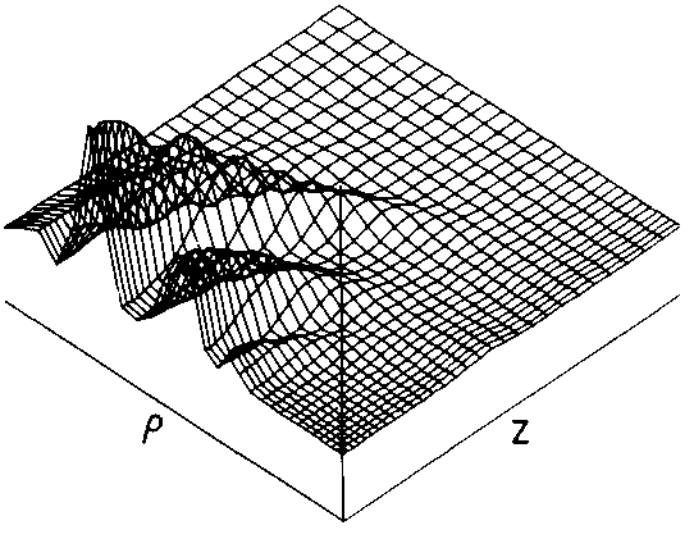


FIGURE 3. The same quantity as in FIGURE 2 except at $t = 5.4$. The "cloud" has dispersed into an outgoing wave train of gravitational radiation. Note there are four pulses, with the middle two the largest.

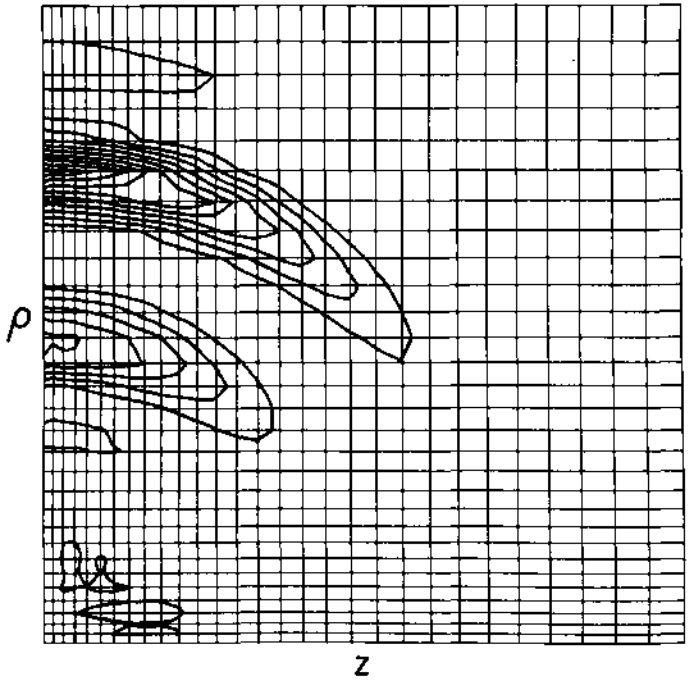


FIGURE 4. A contour plot or $r^2 I$ as shown in FIGURE 3. This clearly shows the quadrupolar nature of the radiation, which should have angular dependence $\sim \sin^4\theta$, where $\theta = 0$ on the z-axis.

r_0, is plotted as a function of time in FIGURE 9. Note that at late times this converges to $\Delta M \simeq 7.3 \times 10^{-8}$.

Taken together these pictures give a complete qualitative view of radiation dispersing from a bounded source. Quantitatively, the problem is more difficult. Because the wave is so weak, the original mass is quadratic in A and must be picked out of the numerically derived conformal factor ψ. Eppley has investigated many ways of calculating the coefficient μ in $M = \mu A^2$, and to date his best value is $\mu = 0.014$. This is consistent with the Bondi mass-loss result since all of the

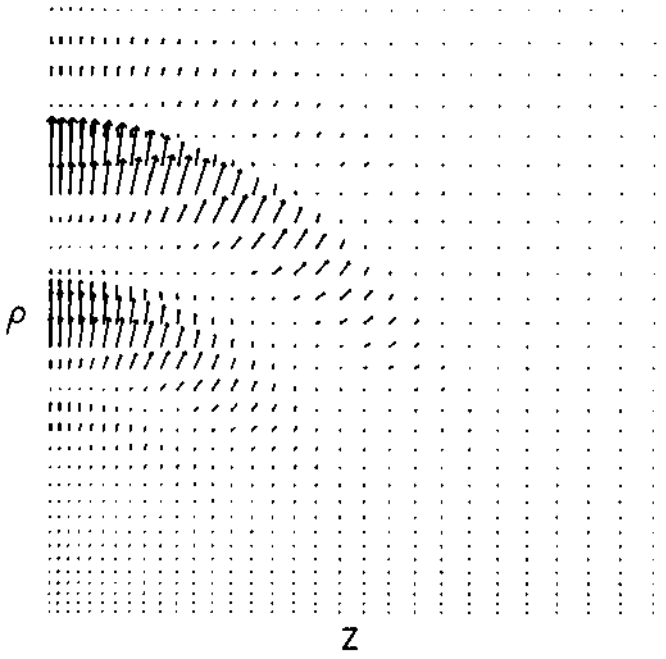


FIGURE 5. Bel-Robinson vector P_i for the same time as FIGURES 3 and 4. The length of the arrow is proportional to a norm $(P_i P^i)^{1/2}$ and the direction is the direction of the vector **P**. This calculation shows convincingly that the Bel-Robinson vector field is able to "locate" gravitational radiation in a space-time.

original mass should pass through the 2-sphere during the clouds dispersal. The value for the Bel-Robinson flux (FIGURE 10) is somewhat lower, leading to a $\Delta M \simeq 6.7 \times 10^{-9}$, again consistent with the order of magnitude. The wavelength $\lambda = 2\pi\omega^{-1}$ used in Equation 31 must be taken from the news function η which is, of course, the distance between every other peak of dM/dt in FIGURE 8. The real problem here is to select a small number accurately. The qualitative picture is impressive, but more hard work needs to be done to get a firm quantitative result.

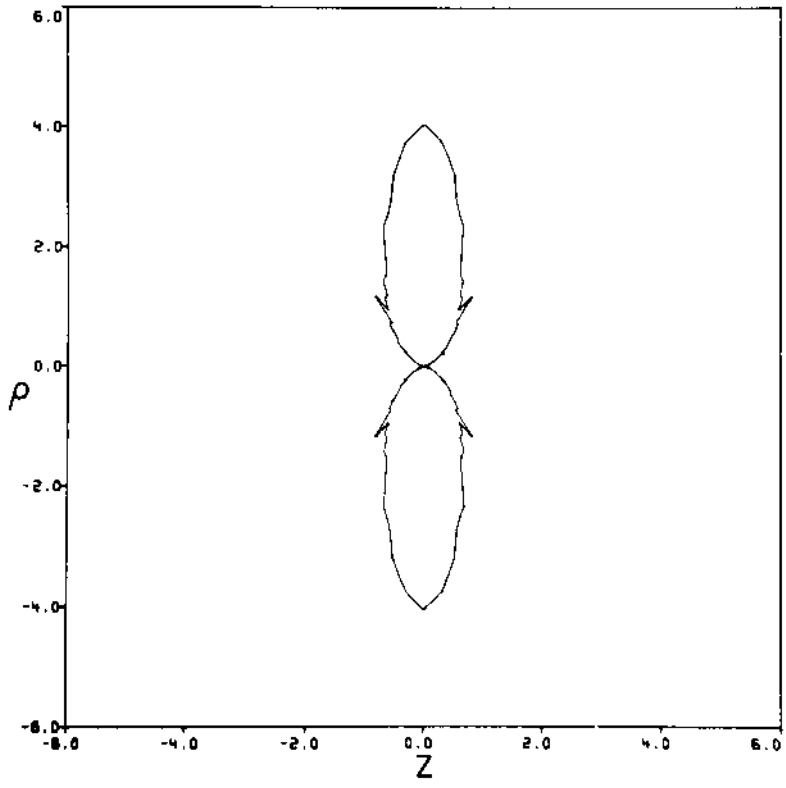


FIGURE 6. The radiation pattern, $dM/dt\,d\Omega$, as measured on a 2-sphere at $r_0 = 3.6$ at time $t = 4.8$. The z-axis is again horizontal, and the equatorial plane (ρ-axis) is vertical. At any angle, the radius vector to the pattern is proportional to the flux of radiation at that moment. The overall scale of the pattern is the logarithm of the instantaneous power dM/dt. Note that at this time (near the maximum power in the fourth pulse) the pattern is largely quadrupolar.

Two Black Hole Collision

Having shown that one can evolve a space-time numerically and obtain useful information about gravitational radiation, I now turn to a more astrophysically interesting scenario. The collision of two black holes is often envisioned as an observable source of gravity waves, the event usually being thought of as occurring in dense nuclei of galaxies or quasars. In general, such a collision would be a near-miss encounter, followed by orbital capture, then a spiraling in, and finally a coalescence. Unfortunately, to calculate this process requires a full three-dimensional dynamical computer code, something which may be achieved in the next few years. As of now, the best we can do is study the head-on axisymmetric collision of two nonrotating black holes (axisymmetric rotation can be added fairly easily).

The most important astrophysical question is: how much gravitational radiation is generated by this time-changing strong gravitational field? Before finding

the actual answer by solving for the space-time, I attempted to estimate the radiation that might be generated.[6] To lowest order one can approximate the collision by two point particles attracted toward each other by Newton's law of gravity and obeying Newton's law of motion. This picture is grossly in error when the relative separation approaches $2GM/c^2$, where M is the total mass. Therefore I will follow the motion only up to that point. The time dependence of the quadrupole moment for the system, $\mu r^2(t)$, where μ is the reduced mass, can be put in the Landau-Lifshitz weak-field theory to obtain the energy radiated in gravitational waves. I have done this calculation analytically, assuming the particles start at rest with separation L_0. The total energy radiated from $r = L_0$ to $r = 2M$ is:

$$\frac{\Delta E}{Mc^2} = \frac{2}{105}\left(\frac{\mu}{M}\right)^2\left(1 - \frac{2M}{L_0}\right)^{3/2}\left[1 + \frac{8}{5}\left(\frac{M}{L_0}\right) + \frac{32}{15}\left(\frac{M}{L_0}\right)^2\right] \tag{35}$$

For the case of infinite initial separation this reduces to the formula derived by Zerilli.[38] He was interested in it because the limit in which one particle is much less

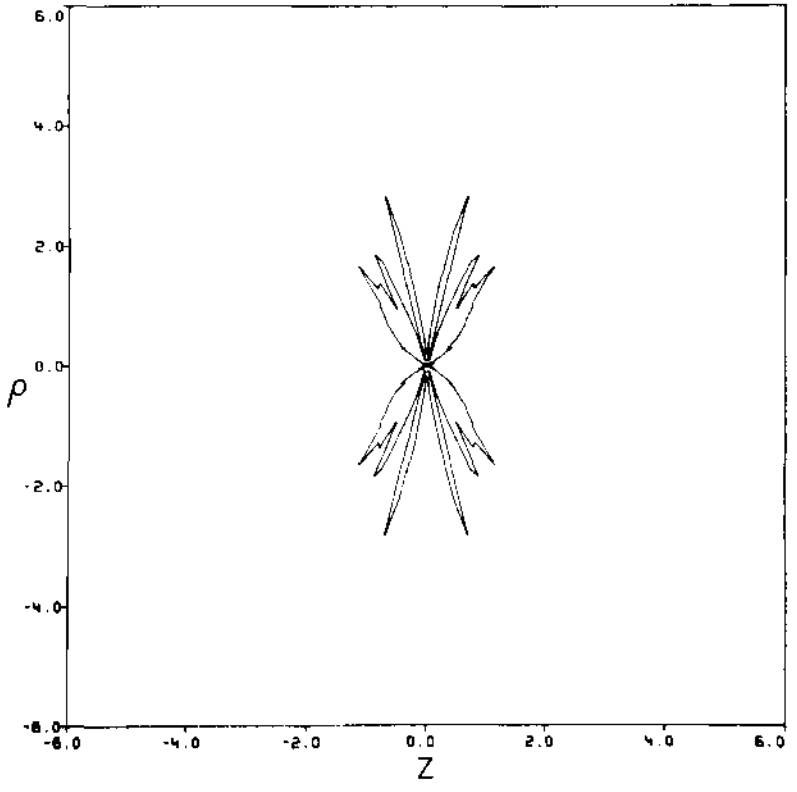


FIGURE 7. The same as FIGURE 6 except at $t = 5.1$. The "spikes" are the higher multipoles which appear when the quadrupole radiation goes through a node. Note they carry a very small portion of the total energy.

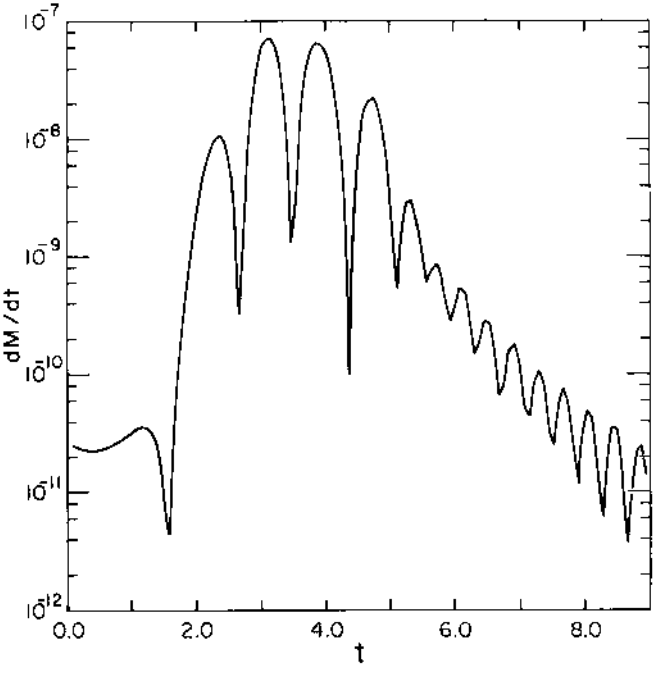


FIGURE 8. The instantaneous power dM/dt, as a function of time t, through the 2-sphere in FIGURES 6 and 7 integrated over angle. The mass loss here is calculated using a modification of the Bondi mass-loss formula (Eq. 27). Note the four main pulses, as seen in FIGURES 3–5, are seen here followed by a ringing down.

massive (μ) than the other (M) should be a first approximation to the fully relativistic problem of dropping a test particle radially into a Schwarzschild black hole. This problem was solved using perturbation theory by Davis, Ruffini, Press and Price[39] in 1971. They found

$$\frac{\Delta E}{Mc^2} = 0.010 \left(\frac{\mu}{M}\right)^2 \qquad L_0 = \infty, \tag{36}$$

approximately one half the amount predicted by the Newtonian calculation. In a followup paper Davis, Ruffini, and Tiomno[40] and later Chung[41] calculated the mass loss from the problem. It is shown in FIGURE 11. Whereas the Newtonian calculation has an ever rising dE/dt as $r \to 2M$, the relativistic calculation finds several peaks.

The above suggests that as a first guess for the two equal mass collision we put $m_1 = m_2 = \frac{1}{2}M$ in Equations 35 and 36. The result is that the Newtonian freefall radiation efficiency for parabolic infall of two equal masses is estimated as[6]:

$$\frac{\Delta E}{Mc^2} \simeq 0.0012 \qquad \text{(Newtonian)}$$

$$\simeq 0.0006 \qquad \text{(Semi-Relativistic)} \tag{37}$$

Now something like this much radiation *must* be produced by the two black hole collision. The big question is: does the interaction of the finite size of the horizons, which was not present in the Davis *et al.*[39] calculation, produce a larger amount of radiation than this?

In a sense, the preceding argument is designed to put a lower bound on the gravitational radiation produced. Upper bounds may also be established if one makes a crucial assumption about the evolution of the initial data. This hypothesis, called Cosmic Censorship,[42] states that any singularities that form to the future of a singularity-free initial data set, must occur inside black holes. If this is true, then Hawking[43] proved that the total surface area of black holes must not decrease with time. If the area were able to remain constant during a collision, then the maximum amount of radiation would have gone to infinity, while any increase in surface area decreases the radiation reaching infinity (part of it goes down the holes).

The problem is, as Thorne[44]and others have argued, that Cosmic Censorship is most likely to be violated precisely in dynamic, highly nonspherical, strong field collapse or collision space-times. Therefore, it is imperative actually to evolve

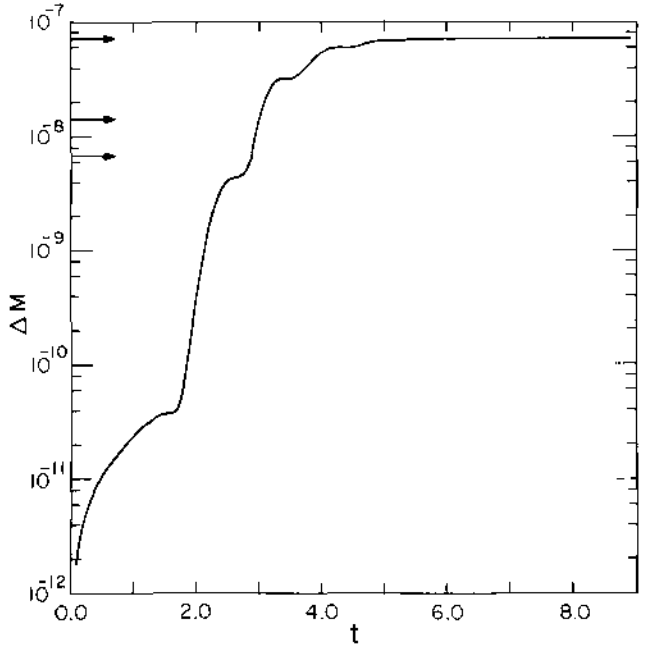


FIGURE 9. The total mass loss, $\Delta M = \int_0^t \dot{M} \mathbf{d} T$, through the 2-sphere of FIGURES 6–8, as a function of time t. Note that at late times this levels off. This value (upper arrow) should equal the total mass (middle arrow) as measured on the initial data. The fact that these do not agree has been traced to an inaccurate numerical preparation of the initial data. The lower arrow indicates the estimate of the mass loss provided by the Bel-Robinson flux (FIGURE 10). This evolution will be refined in future work until these three methods converge.

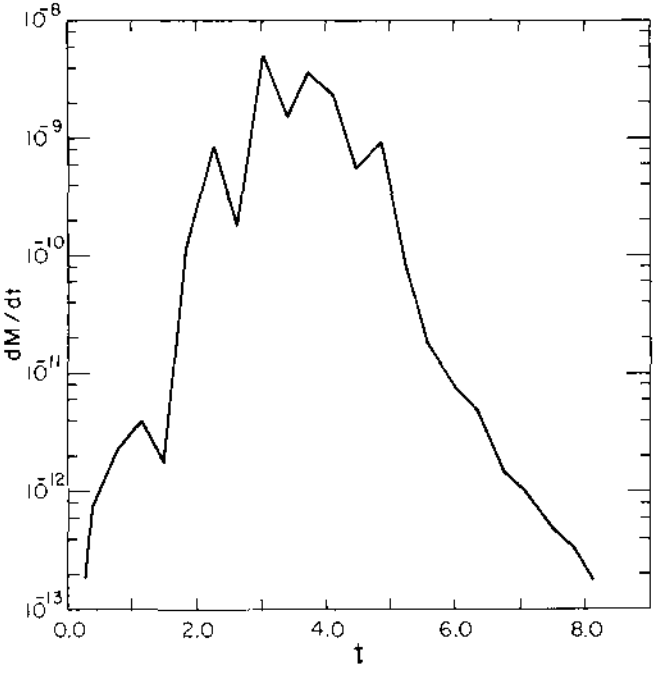


FIGURE 10. The estimate of the instantaneous mass loss using the Bel-Robinson vector (Eq. 31). Note that it agrees qualitatively with the Bondi mass (FIGURE 8), but quantitatively it is 10 times lower. The reason this curve is not as smooth as FIGURE 8 is that we numerically evaluated the Bel-Robinson vector less often than the Bondi mass loss.

such space-times, using only Einstein's equations, to see whether the surface area actually increases. If it does, or alternatively if the radiation reaching infinity is much less than the Hawking upper limit, then this vital hypothesis will have passed a crucial test.

For the time being let us assume the standard picture is correct. Then the upper limit[45] to the energy radiated by gravitational radiation during the collision of two nonrotating black holes dropped from rest at infinity is $0.29Mc^2$. This upper limit comes from assuming the process is reversible in the thermodynamic sense, i.e., that the surface area remains constant during the collision. (It is now well established[46,47] that black hole surface area *is* entropy.) However, it is clear that some radiation will go down the holes during the coalescence phase; this is irreversible and will increase the surface area. A simple calculation shows that the efficiency ϵ for producing radiation goes as:

$$\epsilon \equiv \frac{\Delta E_{\text{rad}}}{2mc^2} = 1 - \sqrt{\frac{A_f}{2A_i}} \tag{38}$$

where A_f and A_i are the final and initial surface areas, respectively. If $A_f = A_i$, then $\epsilon = 0.29$. If $A_f = 2A_i$, the efficiency drops to zero. Therefore, the question of

the efficiency of colliding black holes for producing gravitational radiation can be stated as: how close does the surface area come to doubling during the collision?

Let me now describe the details of the numerical evolution. Since the theoretical framework of this problem has been extensively reviewed[22] recently, I will only briefly mention the major points. As initial data we use Misner's analytic solution[48] of the constraint Equations 10. Metrically the 3-geometry is conformally flat (unlike the Brill data Equation 32) and time symmetric ($K_{ij} = 0$), i.e., the holes start at rest. Topologically, it consists of two Einstein-Rosen bridges[49] joining two identical asymptotically flat 3-spaces. In a realistic astrophysical model, these bridges would be replaced by two pockets of matter[8] inside their event horizons. However, since the details of what is inside the black hole cannot affect the outside, the results on gravitational radiation should be very similar.

There is one dimensionless parameter in the Misner initial data: the separation L_0 of the throats (narrowest part of the bridge) in units of the total mass of the system M. Eppley and I have evolved the initial data for two values of L_0/M, namely 3.88 and 6.60. These values of L_0/M can be used in Equation 35 to estimate the Newtonian radiation for this bound system.

The apparent horizons (outer boundary of trapped surfaces) are at the narrowest part of the two bridges on the initial time surface, whereas the event horizon (the surface of the black holes) lies somewhere outside of the apparent horizons. While one cannot locate the event horizon without knowledge of the full space-time, the apparent horizons can be located on each time slice. Gibbons and

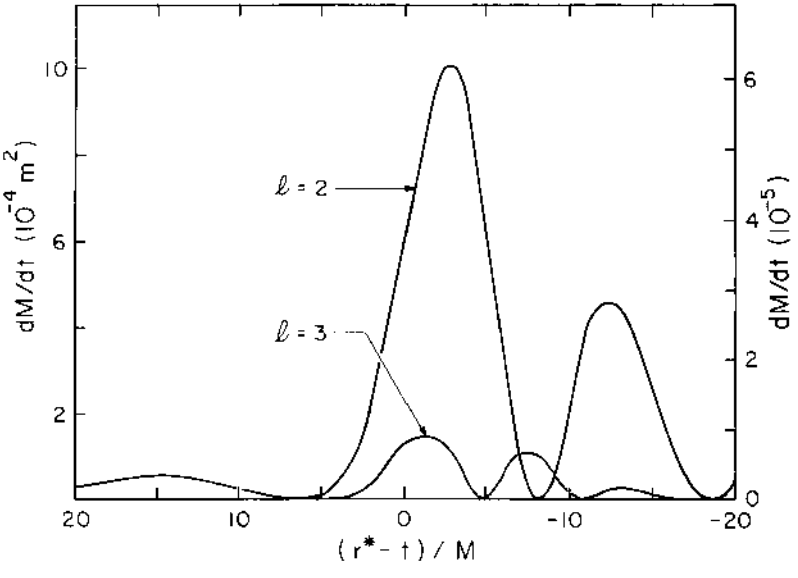


FIGURE 11. The instantaneous mass loss (right-hand scale) due to a small particle (μ) falling into a black hole (M) as calculated by Davis, Ruffini, and Tiomno[40] and Chung.[41] I have scaled this to two equal masses by regarding μ as the reduced mass and M as the total mass ($m \equiv \mu/M \to \frac{1}{4}$). Note the vertical scale corrects an error of a factor of 10 in the original publication.[40]

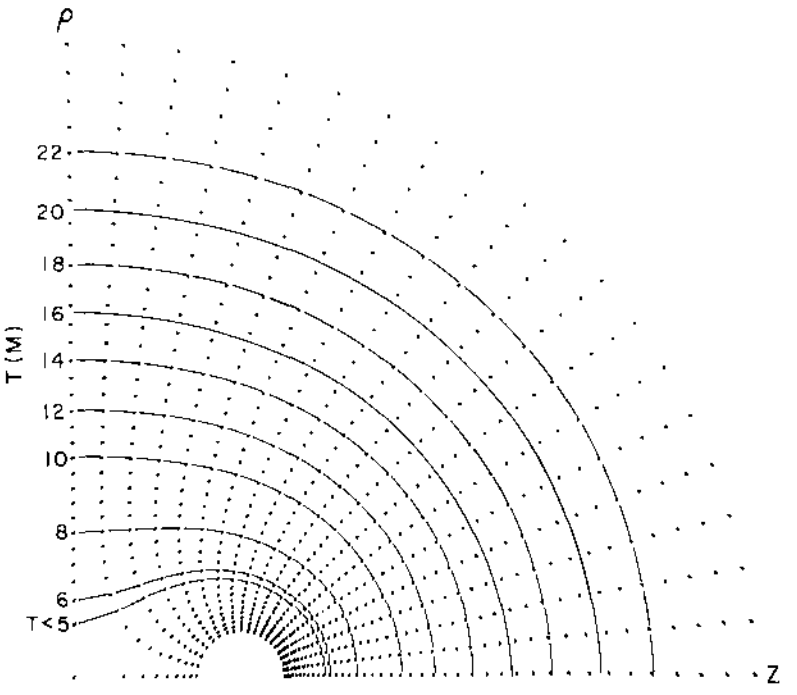


FIGURE 12. The dots are the actual grid points used in the numerical evolution of two colliding black holes. The horizontal axis is the z-axis, while the vertical axis lies in the equatorial plane (ρ-axis). The apparent horizon of the black hole at $t = 0$ lies on the innermost circle of dots. As time progresses the horizon moves outward with respect to the grid points. To estimate the location of the horizon, we assume that the final area of the horizon is $A_f \sim 2A_i$ (i.e., almost no radiation escapes to infinity). Then at each value of time (T/M) there is a coordinate 2-sphere (solid line) which has area $2A_i$. Note the spherical state as late times.

Schutz[50] and Čadež[51,22] have used the area of the apparent horizons to put upper limits on the efficiency of gravitational radiation generation by the collision of these two bound holes (FIGURE 18).

The time slicing we used was the maximal condition, Equation 3. Because of the existence of the throats, boundary conditions on the acceleration potential α must be specified not only at spatial infinity on the upper sheet but also on the throats.[52] We chose $\alpha = 0$ there because this mimics as closely as possible the standard t = constant slices of Schwarzchild. Note that since the event horizon is outside of this boundary initially, it will evolve on the region outside of the throats.

The question arises: how far in time does one need to evolve the data? As a first guess, I used the Newtonian freefall time from L_0 to $r = 2M$:

$$t = \left(\frac{2M}{L_0}\right)^{-1/2}\left[2\sqrt{\frac{1 - 2M/L_0}{2M/L_0}} + \left(\frac{L_0}{M}\right)\tan^{-1}\left(\sqrt{\frac{1 - 2M/L_0}{2M/L_0}}\right)\right] \quad (39)$$

which is $7M$ for $L_0/M = 3.9$ and $17M$ for $L_0/M = 6.6$. We carried our evolution to $t = 22M$ for the former case and $t = 31M$ for the latter, so we should have safely integrated past the collision time.

To "see" the actual collision one would like to solve for the location of the apparent horizon on each time slice. Even more ambitiously, one could track null rays through the space-time lattice and find which ones escape, thus locating the actual event horizon. Although both are numerically feasible[53] we have not yet had time to implement these procedures. However, there is a poor man's guide to watching horizon development. Assume that $\Delta E_{\text{rad}}/Mc^2 \ll 1$ and that $A_f \simeq 2A_i$. (This will be justified below). Then at each time we can ask which coordinate 2-sphere has proper area A_f.

Eppley and I did this, and the result for $L_0/M = 3.9$ evolution is shown in FIGURE 12. The grid points represent the lattice sites at which quantities were evolved. The initial apparent horizon with area A_i is shown at $t = 0$. Until $t \simeq 5M$, the surface labeled "$t < 5$" has area $2A_i$. After $t \simeq 5M$, the 2-surface of area $2A_i$ begins moving out with respect to the grid. This outward motion is just what one finds for the maximal slicing of a Schwarzschild black hole[7] ("the grid is sucked down the hole").

Now it would be useful if one could actually locate the apparent horizon at late times, since it would be very near the actual event horizon and its surface area A_f could be used to measure the gravitational radiation loss (Equation 38). Unfortunately, I feel this will never be a quantitative help. FIGURE 13 shows the radial proper metric function at late times ($t = 20M$). The initial conformal factor in the line element has been factored out so that this metric function was unity (flat) at $t = 0$. The peak is characteristic[10] of the proper radial metric

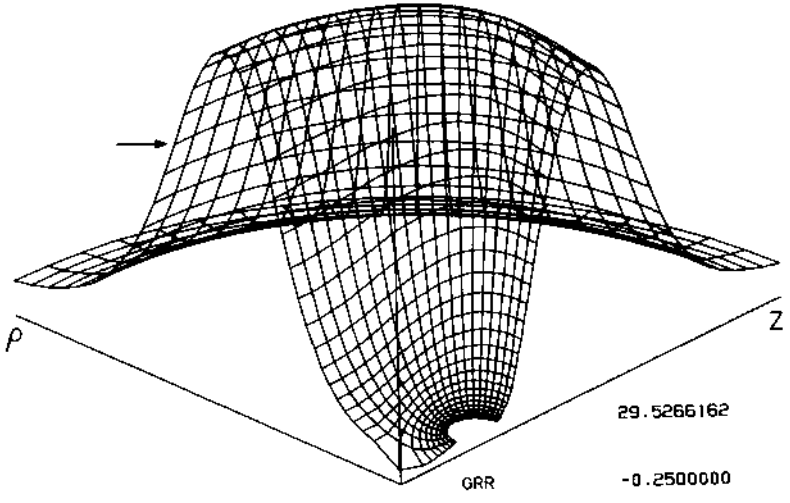


FIGURE 13. The relative change in the radial metric function g_{rr} at late times ($T \sim 20M$). Note the peak which is approximately spherically symmetric. The arrow shows where the horizon is for a similar evolution of a single spherical black hole. This agrees quite well with FIGURE 12.

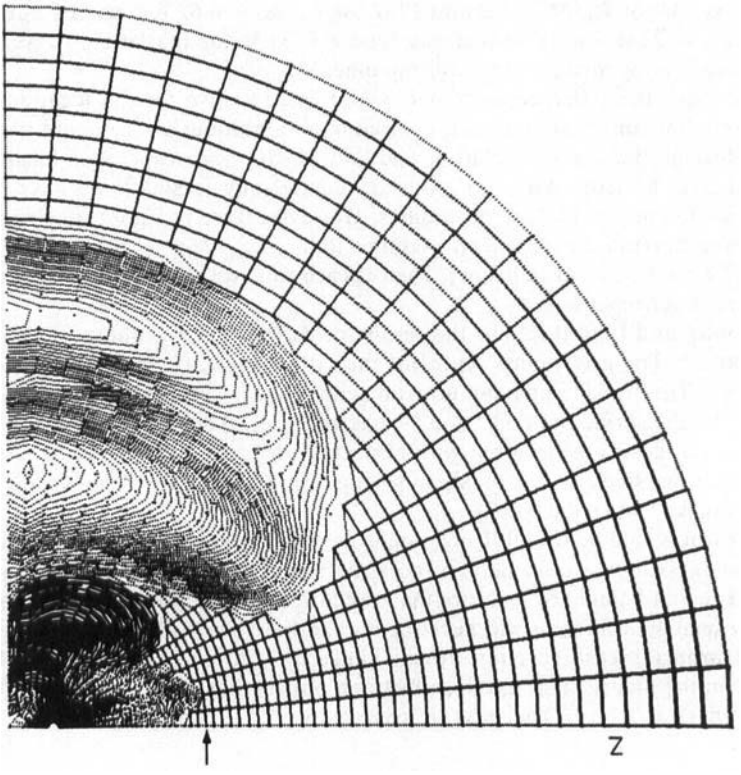


FIGURE 14. A contour plot of the radial component of the Bel-Robinson vector at $t \sim 20M$ for the $L_0/M = 6.6$ collision. Note the similarity in the pulses of outgoing radiation with those in FIGURES 4 and 5. The dotted lines represent outgoing radiation, the solid lines ingoing radiation. The location of the 2-sphere on which mass-loss was measured is shown by an arrow.

function for maximal slicing of a spherical Schwarzschild black hole. In that calculation one knows where the horizon is—it occurs slightly outside the peak. The arrow points to the coordinate 2-sphere whose area is $2A_f$ at this time. Its location is quite consistent with our experience from Schwarzschild. However, if the actual horizon is on the 2-sphere just one radial grid line inward, its area is sufficiently less than the efficiency from Equation 38 would be 5% instead of 0%. Since the actual efficiency seems to be $\ll 1\%$, it is unlikely that locating the horizon numerically will be accurate enough to measure the mass loss reliably.

To attempt to get an estimate of the efficiency, Eppley and I first evaluated the Bel-Robinson vector field for the collision space-time. In particular, since the energy flux depends only on the radial component P^r, Equation 31, this quantity was evaluated at each grid point. If only the physical red shift were present, then $\oint P \cdot dS$ would presumably decrease as one followed a wave outward from its formation close to the strong field region, until the integral reaches a steady value, proportional to $\dot{M}$, in the wave zone. Unfortunately, the inherent numerical

dissipation in our differencing scheme begins to damp out the waves as they enter the wave zone, and thus $\oint P \cdot dS$ decreases as the waves propagate outward.

A contour plot of the logarithm of P^r is shown in FIGURE 14 for the $L_0/M = 6.6$ collision. One "sees" very clearly the gravitational waves which have already been generated (compare FIGURE 4 for Brill waves). Since this "snapshot" is at $t = 20M$, just about the expected time of collision from Equation 35, this illustrates that some of the radiation is generated *before* the collision, i.e., during freefall. In the movie containing this frame, one can also observe the time development of the central region. Very little of interest occurs until collision time, at which point the "jet" of heavy contour lines boils out of the coalescence region. This "splat" represents a region in which the P^r is *inward* pointing. Presumably, the near-zone features are rather coordinate and slicing dependent, but at least this feature seems related to the physical collision.

We used several coordinate 2-spheres to measure the Bel-Robinson flux and the modified Bondi mass-loss. The most useful quantitative information seemed to come from a 2-sphere whose areal radius $r = \sqrt{A/4\pi}$ was $8M$ at $t = 0$ (shown by arrow in FIGURE 14). This was chosen because it was close enough in that most of the waves propagated out to and through the 2-sphere by the time our calculation stopped, and because the numerical dissipation was not as strong here as it is further out. The problem is that $r = 8M$ is still fairly close to the holes so our use of Equation 31, which gives the energy flux at $r = \infty$, probably has errors of order unity.

In any case, FIGURE 15 shows the energy flux derived from the Bel-Robinson

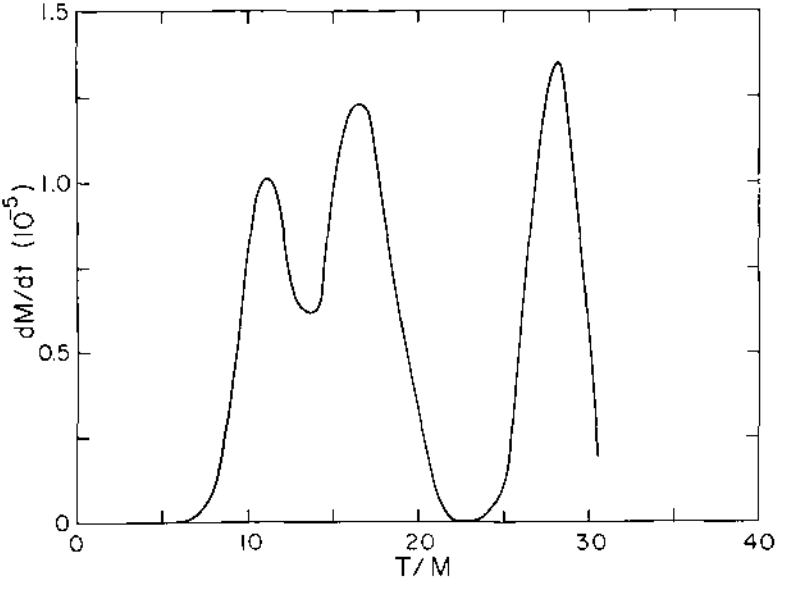


FIGURE 15. The instantaneous mass loss as a function of time (T/M), through the 2-sphere shown in FIGURE 14, given by the Bel-Robinson vector.

flux using Equation 31. The wavelength λ was estimated to be $\lambda \simeq 24M$ from the Bondi mass flux (FIGURE 16). To obtain the Bondi mass-flux a trick was required. Because the 2-sphere was a fixed *coordinate* 2-sphere, its area changes with time. In particular, its area decreases as the maximal slicing with zero shift vector forces the radial coordinates to be sucked into the hole (FIGURE 12). As the 2-sphere falls through the gravitational field, it picks up a false octupole radiation pattern (FIGURE 17). For this reason, I assumed a $\sin^4\theta$ quadrupole pattern for the real radiation and used the news function on the equator, $\eta(\theta = \pi/2)$ to set the scale. This procedure applied to the Brill gravitational waves gave results for $\dot{M}$ essentially indistinguishable from the method of integrating the actual pattern over the 2-sphere.

The result is shown in FIGURE 16. Note that the Bel-Robinson flux agrees with the Bondi flux as regards the timing of the main pulses, just as we found for the Brill waves. (The fine-structure difference is not real since an Isaacson average[29] should be done to localize the energy.) Much more interesting is the basic agreement on the wavelength and structure of pulses with the Davis *et al.*[39] calculation of a small particle falling into a large one (FIGURE 11). Quantitatively, the scaled Davis *et al.*[39] calculation yields a larger number for $\dot{M}$ than either Bel-Robinson or Bondi, but all have $\dot{M} < 10^{-4}$ for all t. This would seem to imply that "in-flight" radiation[6] is the dominant radiation produced by the two black hole collision up to $t \simeq 20M$.

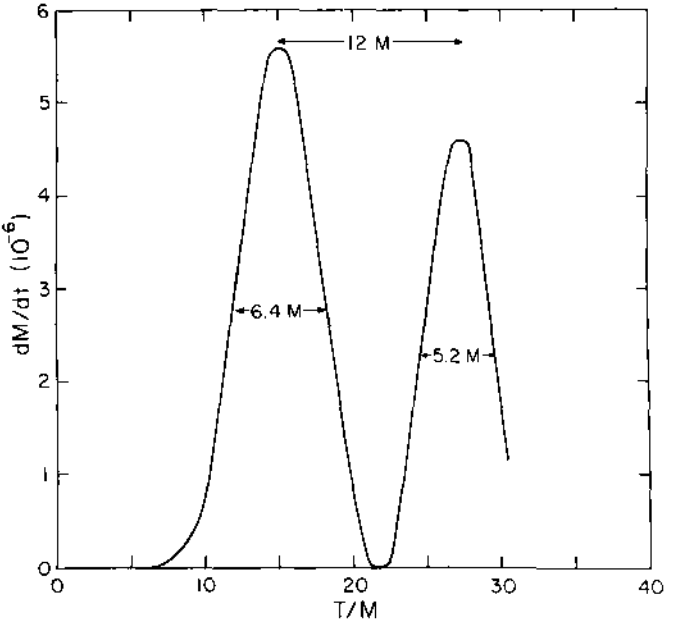


FIGURE 16. The same as in FIGURE 15 except using the modified Bondi mass-loss formula. Note the very striking qualitative agreement with the scaled version of the unequal-mass perturbation calculation[40,41] shown in FIGURE 11. The quantitative dissagreement is mainly due to the artificial damping of our differencing scheme.

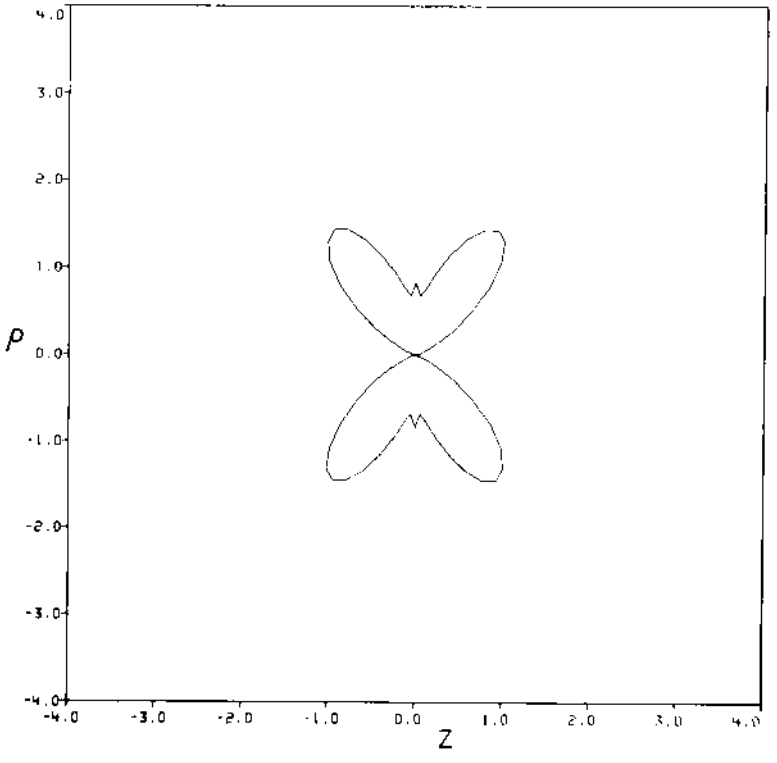


FIGURE 17. The radiation pattern, $dM/dtd\Omega$, on the 2-sphere at fixed coordinate radius. Because this 2-sphere is "sucked toward the black hole" by the maximal slicing condition with zero shift vector, the proper radius of this 2-sphere decreases with time. Here at $T = 16.6M$, for the $L_0/M = 6.6$ collision, the proper radius is $\sim 8.1\,M$. The octupole pattern is presumably caused by the 2-sphere falling through the gravitational field, while the pattern near the ρ-axis ($\theta = \pi/2$) is caused by outgoing quadrupole radiation.

Integrated over time, the values for the efficiency ϵ are shown in FIGURE 18. These numbers must be treated as preliminary, because both our theoretical formulae and our numerical scheme are somewhat shaky. Furthermore, there presumably is more radiation to come off the collision. Therefore, I have left an order of magnitude uncertainty above the higher answer given by either Bel-Robinson or Bondi. Nonetheless, I think it is clear that the efficiency for generation of gravitational radiation by head-on collision of nonrotating black holes is very low and consistent with the Newtonian calculation $\epsilon \simeq 10^{-3}$.

This is two or three orders of magnitude lower than the Hawking-type upper limits which assume a reversible (no change of surface area) collision. Our calculations indicate the collision is very irreversible with $A_f \simeq 2A_i$ in Equation 38. There seem to be several reasons why this is so. FIGURE 19 shows an isometric embedding diagram of the $z - \rho$ plane of the $t = 0$ and $t = 9M$ slices of the $L_0/M = 3.9$ collision. The $t = 9M$ diagram represents the geometry immediately after coalescence. As can be seen, there is very little dramatic difference between

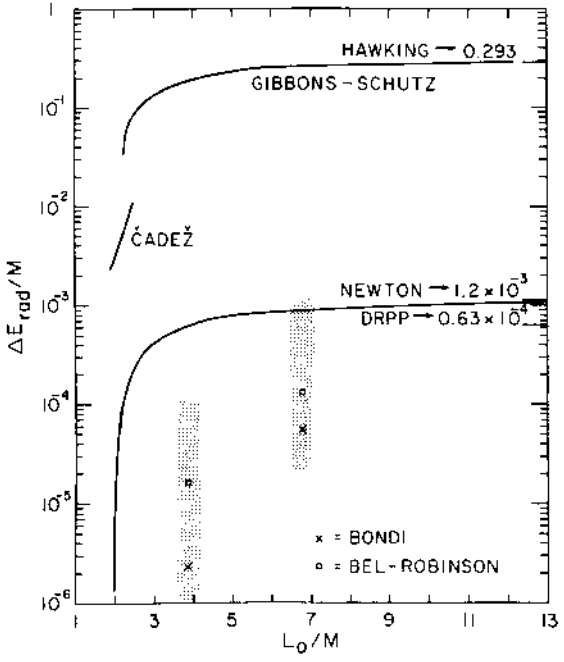


FIGURE 18. Various techniques have been used here to estimate the efficiency for generating gravitational radiation, $\Delta E_{rad}/M$, from the head-on collision of equal mass black holes ($m_1 = m_2 = \frac{1}{2}M$). The horizontal axis is the initial separation of the apparent horizons. Upper limits using black hole area theorems due to Hawking, Gibbons and Schutz, and Čadež are shown. The estimate provided by the Newtonian-Landau-Lifshitz weak field, slow motion, method is given by the lower solid line. On the right, the limits for $L_0/M \to \infty$ are written, including the scaled DRPP[39] result (see FIGURE 11). Finally, the preliminary computer results for the actual collision are marked in the shaded region. The answers obtained by the Bondi and Bel-Robinson techniques are specified together with a guess at the probable error boxes. Subsequent computer evolutions will greatly improve the accuracy of these results.

the two times. The neck stretches (as observed in the Schwarzschild maximal slicing) and it is constricting where the new horizon is forming around the two throats (see FIGURE 12). However, if the coalescence were going to produce a large amount of gravitational radiation, it would be necessary for a rapid time variation of the 3-geometry to occur.†† This does not happen—the holes "ooze" together.

Even if "radiation" were to be generated by the horizon coalescence, it would have to fight a tremendous gravitational red shift. If, by the time the wave reaches $r_0 \simeq 3M$, its wavelength is greater than $\sim 16M$, then it will be reflected back into the hole by the curvature potential barrier which occurs in the perturbation calculations.[54] Since both of these arguments are somewhat generic, I believe that horizon coalescence in general will be a poor generator of gravitational radiation.

There is a situation in which a head-on black hole collision is efficient at generating gravitation radiation: an extremely hyperbolic collision ($v_\infty \simeq 1$). D'Eath[55] has recently calculated the details of such a collision, and he finds $\epsilon = \Delta E_{rad}/2m\gamma c^2 \to 0.25$ as $v_\infty \to 1$. This is consistent with the estimates made by applying a simple technique called the Zero Frequency Limit (ZFL).[56] Using D'Eath's exact value for $\epsilon(v_\infty = 1)$ to fix the numerical factor in the cutoff frequency ω_c of the frequency spectrum $dE/d\omega$, I find the following estimate of ϵ,

††I thank Charles Misner for suggestions on this interpretation.

using ZFL for hyperbolic head on collisions:[56]

$$\epsilon = 0.122 \left\{ 2 + (1 - v^2) \left[1 - \left(\frac{3 + v^2}{2v} \right) \ln \left(\frac{1 + v}{1 - v} \right) \right] \right\} \tag{40}$$

Evaluation of this formula (see FIGURE 20) shows that ϵ drops below 1% by the time $v_\infty \lesssim 0.5$. For lower values of v_∞, the ZFL underestimates the actual effi-

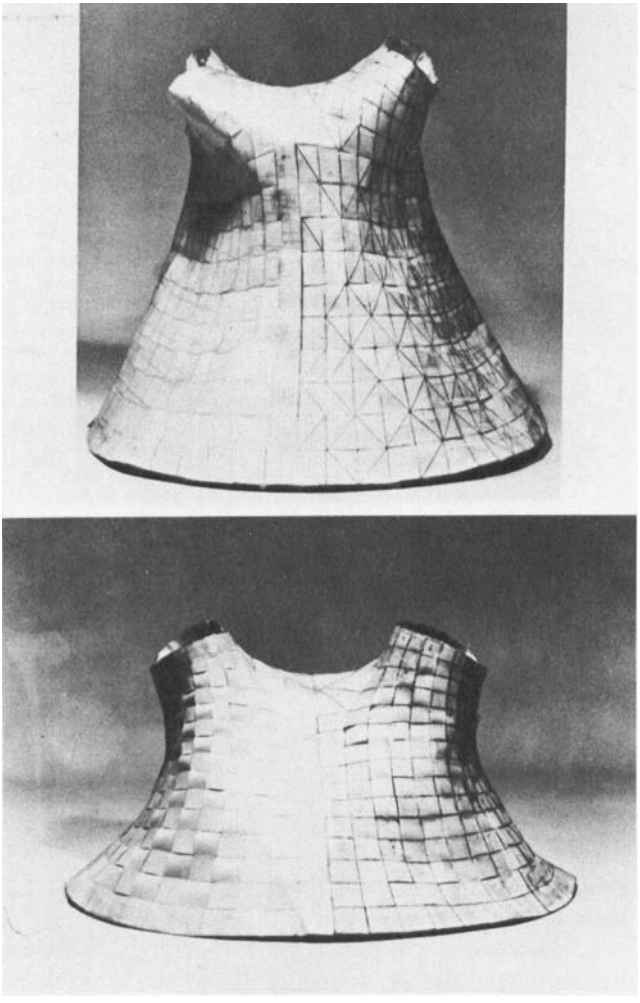


FIGURE 19. These isometric embedding diagrams of the z-ρ plane were constructed at the Center for Relativity in Austin, Texas, using a program written by Tom Criss. They show the two black holes at $t = 0$ (lower) and $t = 9M$ (upper) for the $L_0/M = 3.9$ collision. The shearing at the grid can be seen clearly. The geometry stretches as in Schwarzschild[7] and constricts where the new horizon is forming.

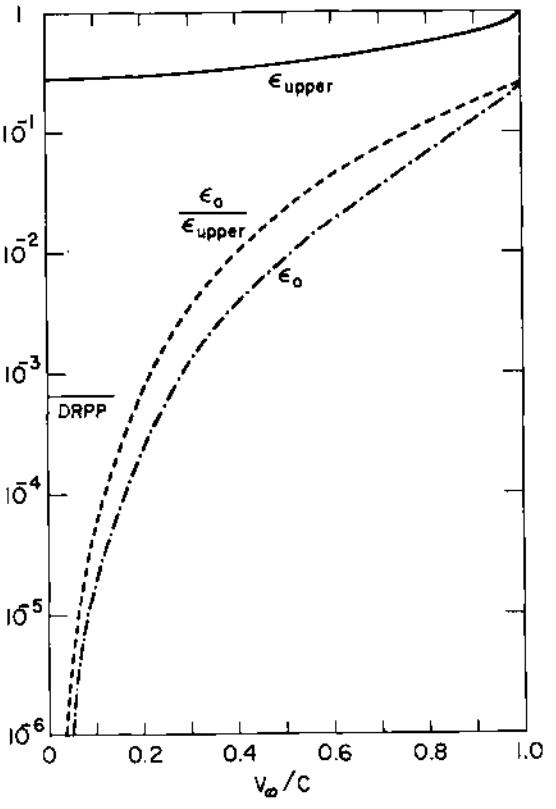


FIGURE 20. Estimates on the efficiency, $\Delta E_{rad}/2m\gamma c^2$, for hyperbolic head-on collisions of black holes. The vertical scale is dimensionless while the horizontal scale gives the velocity at infinity v_∞/c. The solid upper line, ϵ_{upper}, is the upper limit obtained from using an area theorem. The lower line, ϵ_0, is derived by use of the ZFL[56] technique. This should give the actual efficiency for $v_\infty/c > 0.5$ and underestimate it for lower v_∞. The value of $\epsilon_0 = 0.25$ for $v_\infty/c = 1$ is due to D'Eath.[53] Notice that ϵ_0 estrapolated to $v_\infty = 0$ is consistent with the DRPP result for parabolic infall. The ratio of the actual efficiency to the upper limit, $\epsilon_0/\epsilon_{upper}$, decreases rapidly with v_∞/c, which implies that the collision is more irreversible for lower v_∞.

ciency because the low frequencies no longer dominate the spectrum. Using instead a simple extrapolation of the ϵ_0 curve for high v_∞ (FIGURE 20) one finds a result quite consistent with $\epsilon \lesssim 10^{-3}$ for $v_\infty = 0$.

One can compare this estimate of the actual ϵ with the upper limit obtained by a naive use of the Hawking argument:[6,22]

$$\epsilon_{upper} \lesssim 1 - \frac{1}{\gamma\sqrt{2}}. \tag{41}$$

(Although this gives $\epsilon_{upper} \to 1$ as $v_\infty \to 1$, Penrose[60] has shown by use of method analogous to Gibbons and Shutz,[52] that $\epsilon_{upper} \to 0.5$.) In any case, if the black hole surface area did not increase during the collision, ϵ_{upper} would be of order ~0.5 for any hyperbolic collision. Equation 40 above, however, indicates the actual efficiency drops rapidly for $v_\infty < 1$. The ratio $\epsilon/\epsilon_{upper}$ (FIGURE 20) thus gives a measure of how irreversible the collision is. This tells us an important new fact: black hole collisions are *more irreversible* the smaller the velocity (v_∞) is at infinity. This is unfortunate for gravity wave astronomy, because it is unlikely that the more efficient hyperbolic collisions occur in nature.

Other Sources of Gravitational Radiation

As mentioned earlier, head-on collisions will be very rare events, the more usual case being a spiral collision. As the compact objects (neutron stars or black holes) orbit, they will radiate away the change of binding energy in gravity waves. This will continue until the objects collide, tidally disrupt, or reach an unstable circular orbit from which they plunge to a collision in less than one orbit. Recently, Clark and Eardley[58] have analyzed such a scenario for two neutron stars. (For a black hole-neutron star collision see Ref. 59). They find that typically the gravitational wave efficiency is $\epsilon \sim 2\%$. Now the important point is that this high efficiency is just due to the Newtonian binding energy, not an esoteric strong field effect.

In fact, it seems likely to me that not much more will come out if two black holes are involved.[60]‡‡ The reason is that the holes probably plunge after the binding energy is $\sim 0.05\, Mc^2$. The experience with gravitational synchrotron radiation[61,62] indicates most of the plunge radiation also goes down the hole. Finally, if my argument that horizon coalescence is inefficient is generic, then little will come off from the collision.

There are four astrophysical situations where such spiral collision may be found. First, normal binary systems may evolve to contain two compact objects (such as PSR 1913 + 16), and then this system may decay[63] to a spiral collision[64] on a time scale of $\sim 10^8$ years. Second, if relativistic clusters of collapsed objects form in galactic nuclei or quasars, the captures[65,66] of compact objects may be fairly frequent. Alternatively, these active regions may contain collapsing supermassive stars which fission and form two supermassive black holes which later collide.[67] Fourth, normal stellar cores may be rotating rapidly enough that they fission after collapsing to form a neutron star.[68] All of these cases can be modeled by a fully three-dimensional computer code,§§ as mentioned earlier.

Astrophysically, there are very real difficulties with these events being observed by the next generation of gravity wave detectors. The first case is far to rare[58] to yield one event/year even if one can see the Virgo cluster. It is not known whether relativistic clusters ever form, or if they do what their lifetime is. Although Thorne and Braginsky[69] have proposed looking for the second and third cases with precision tracking of interplanetary spacecraft, Rees[70] has given reasons to suggest this may be very difficult because of the astrophysical properties of supermassive stars. Let me finish then, by examining rotating stellar collapse in more detail.

As reported at this meeting by Taylor,[71] pulsar statistics indicate that a neutron star forms about once in 10 years per galaxy. Thus, the collapses in nearby galaxies (out to M101) could be used to give event rates[1] of ~ 1/yr. The question is: what is the efficiency in a typical collapse? In an attempt to answer this question, Thuan and Ostriker[72] studied the collapse of dust spheroids to pancakes, using the Newtonian results of the time rate of change of quadrupole moment to estimate the

‡‡Zel'dovich and Novikov,[60] on p. 110, estimate $\Delta E_{\rm rad} \sim 0.02\ (\mu^2/M)$ for a head-on collision and $\Delta E_{\rm rad} \sim 0.06\ \mu$ for a spiral one where μ is the reduced mass and M is the total mass.

§§J. R. Wilson and coworkers have succeeded in following a Newtonian collapse and fission on the computer—private communication, 1976.

gravitational radiation loss. Their result[72] is shown in FIGURE 21. As one can see, the maximum efficiency is $\sim 2 \times 10^{-4}$, and this occurs only for cores rotating rapidly enough that the neutron star is rotating near breakup at formation.

Novikov[73] then pointed out that if pressure is included, the radiation emitted during the bounce will be greater than the Thuan-Ostriker result by approxi-

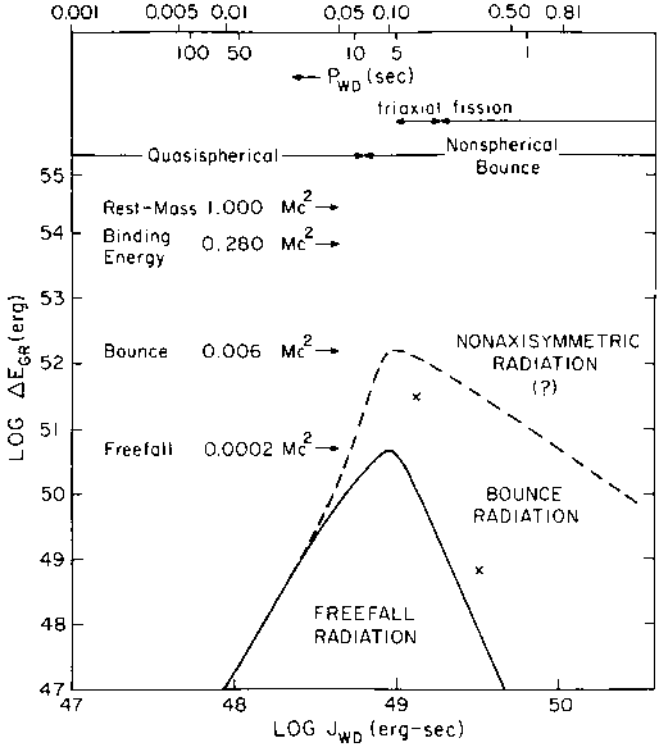


FIGURE 21. Estimates of gravitational radiation efficiency for neutron star formation based solely on Newtonian calculations. The vertical axis gives the energy radiated by the collapse of a 1.4M⊙ rotating white dwarf core with density $\rho \sim 10^9$ g cm^{-3}. The horizontal axis records the initial angular momentum of the core, or alternatively (top scale) the initial eccentricity and period of the core. The final state of the neutron star (assumed to be 1.4M⊙ at $\rho \sim 10^{15}$ g cm^{-3}) is labeled across the top.[82] The solid line is taken from Thuan and Ostriker's[72] paper for axisymmetric dust collapse. The dotted line is an estimate for axisymmetric collapse with pressure based on Novikov's[73] argument. The "x" marks the peak for cold equations of state (upper) and hot equations of state (lower) as obtained by Shapiro.[74]

mately A_b/C_b where A_b and C_b are the semi-major and semi-minor axes of the spheroid at bounce. While this seems like a big improvement, it turns out that the maximum effect occurs when $A_b/C_b \sim 10$. I have estimated the bounce radiation by using Thuan and Ostriker's unpublished numerical results and taking their A/C when $\rho = 10^{15}$g cm^{-3} (see FIGURE 21). This shows the best case still has

$<1\%$ and again only for neutron stars rotating near breakup. Shapiro[74] and others have recently made more detailed calculations which confirm the above rough analysis.

There are a number of further reasons for pessimism about whether realistic *axisymmetric* collapse yields observable gravitational waves. In a real stellar collapse neutrino processes will be of dominant importance. As Kazanas and Schramm[76] have shown, it appears that neutrinos are many times more effective at damping out small deviations from spherical symmetry than are gravity waves. Furthermore, the core does *not* freefall after the onset of inverse beta decay, but rather collpases much more slowly[77] because of the remnant electron and neutrino degeneracy pressure. Computer calculations[78] of realistic spherical collapse suggest that the "bounce" may occur at 10^{13} g cm^{-3} rather than 10^{15} g cm^{-3}. (This effect is very sensitive to the equation of state– Arnett, Schramm, and Wilson, private communication.) All of these factors degrade the gravitational wave efficiency. It should be noted, however, that there are some relativistic effects which enhance gravitational radiation in slowly rotating collapse.[79]

From my experience with the two black hole collision, I would be surprised if these Newtonian results are far off from the fully relativistic ones. In particular, Eardley[75] finds a Hawking type $\epsilon_{\text{upper}} \sim 0.03$ using initial data sets for marginally bound nonspherical axisymmetric collapse. If this limit overestimates the actual efficiency by as many orders of magnitude as occurs in the two black hole collision, then the actual efficiency will be consistent with the above Newtonian results.

A number of workers‖‖ are now calculating the fully relativistic perturbations from spherical collapse. Several other researchers## are building codes which will generalize the techniques successfully used in the Brill wave and black hole collision evolutions to calculate the full nonlinear axisymmetric Einstein-matter equations for stellar collapse. Therefore, we should know within a few years if the efficiency ϵ_0 is indeed $\ll 1\%$ for most axisymmetric collapses. If it is, then since the flux[80] will be $\sim \epsilon_0 M 10^{-6}$ GPU (in order to get an event rate > 1/year), observation by the next generation of gravity wave antennas will be essentially impossible.[1,81]

If, on the other hand, the typical electron degenerate core of massive stars is rapidly rotating ($J > 10^{49}$ g cm^2 sec^{-1}; $M \sim 1.4 M_\odot$) there will not be a stable final neutron star configuration.[82] In this case, in addition to the gravity waves from the above consideration, there will also be many more generated by the triaxial or fissioning core, together with its recollapse.[68] Although no reliable dynamical calculations have yet been made, it seems likely that a gravitational wave efficiency of $\epsilon_0 \sim .05$ could be achieved in this *nonaxisymmetric* scenario. Neutrinos may still be very important here in suppressing gravitational waves.[83] Only a fully relativistic three-dimensional calculation can decide what the ratio of $\Delta E_{\text{neutrinos}} / \Delta E_{\text{gravity waves}}$ is in the collapse of a core with mass M and angular momentum J. This is one of the most important outstanding theoretical problems in relativistic astrophysics.

What I want to stress is that, given the difficulties in either the event rate

‖‖Cunningham, Liang, Monerief, Price, Sengupta, Turner, Wagoner, and Walton.
##Chrzanowski, Gunter, Hoffman, Pachner, Smarr, and Wilson.

or the efficiency of other sources (supermassive stars, relativistic clusters, black hole formation, etc.), it may be that the existence of a viable gravity wave astronomy is equivalent to answering the question: do neutron stars typically form rotating near breakup velocity ($\Omega \sim 10^4$ sec^{-1})? Ruderman[84] in a 1972 survey concludes that they do *not*. Others have argued that they do and that complicated interactions of the pulsar's magnetic field with the supernova envelope may drain off much of the angular momentum and energy of the rapidly rotating core.[85,86] This disarray of opinions carries over into the related question of whether white dwarf cores are rotating fast enough[87] ($P \sim 10$ sec) to form a rapidly rotating neutron star after collapse. I would like to emphasize very strongly to the astrophysicists that these two questions are of vital importance for gravity wave astronomers. On the other side of the coin, the gravity wave astronomers may be soon able to help answer these questions for the astrophysicists: if pulses from neutron star formation are observed then it will be very likely that the compact object is rapidly rotating at birth.

Unfortunately, if these pulses are not observed a definitive answer will not be obtained. That is why both observations and theoretical calculations in neutrinos, stellar evolution, electromagnetic and gravitational radiation, and cosmic rays are all needed to solve this outstanding problem. I believe the work reported herein is a step in this direction.

Acknowledgments

Much of the work presented here is the result of close collaboration with K. Eppley. I have benefited in writing this report by conversations with D. Arnett, D. Brill, R. Chin, P. D'Eath, S. Deser, D. Eardley, S. Hawking, J. Leblanc, C. Misner, J. Ostriker, R. Penrose, W. Press, R. Price, M. Rees, D. Schramm, S. Shapiro, P. Sommers, J. A. Wheeler, J. Wilson and J. York. This work was partially supported by the National Science Foundation at the following universities: Harvard, Maryland, Princeton, North Carolina, and Texas. Further financial support was provided by the Mattern Theoretical Physics Fund of U.N.C., the Richard N. Lane Scholarship at U.T., and by the Harvard Society of Fellows. The very generous support of Lawrence Livermore Laboratories has made many of these computer calculations possible. Finally, let me thank B. S. DeWitt, whose original inspiration led me to this project.

References

1. Thorne, K. S., 1976. Preprint OAP-462, Kellogg Radiation Laboratory, California Institute of Technology, Pasadena, California.
2. DeWitt, C. & B. S. DeWitt, Eds. 1973. Black Holes. Gordon and Breach. New York.
3. Robinson, D. C. 1975. Phys. Rev. Lett. **34:** 905.
4. Wilson, J. R. 1975. Preprint UCRL-76967. Also see 1975. Ann. N.Y. Acad. Sci. **262:** 123.
5. Press, W. H. 1973. Ann. N.Y. Acad. Sci. **224:** 272.
6. Smarr, L. L. 1975. Ph.D. thesis. University of Texas at Austin.
7. Estabrook, F., H. Wahlquist, S. Christensen, B. DeWitt, L. Smarr & E. Tsiang. 1973. Phys. Rev. D. **7:** 2814.

8. Lichnerowicz, A. 1944. J. Math. Pure Appl. **23:** 37.
9. Choquet-Bruhat, Y., A. E. Fischer & J. E. Marsden. 1976. Paper presented at the Enrico Fermi International School of Physics, Varenna, Italy, July, 1976.
10. Eppley, K. R. 1975. Ph.D. thesis. Princeton Univ.
11. Eppley, K. R. 1976. Unpublished work.
12. Eardley, D. M. & L. L. Smarr. 1976. Unpublished work.
13. Wheeler, J. A. 1964. *In* Relativity, Groups, and Topology. edited by C. DeWitt & B. DeWitt, Eds. Gordon and Breach. New York.
14. York, J. W., Jr. & L. L. Smarr. 1975. Bull. Am. Phys. Soc. **19:** 68.
15. Smarr, L. L. & J. W. York, Jr. 1977. Preprint: "Kinematical Conditions in the Construction of Spacetime."
16. Arnowitt, R., S. Deser & C. W. Misner. 1962. *In* Gravitation: An Introduction to Current Research. L. Witten, Ed. John Wiley and Sons. New York.
17. O'Murchadha, N. & J. W. York, Jr. 1974. Phys. Rev. D **10:** 428.
18. York, J. W., Jr. 1973. J. Math. Phys. **14:** 456.
19. Smarr, L. & B. S. DeWitt. 1973. Bull. Am. Phys. Soc. **18:** 643.
20. DeWitt, B. S. & C. W. Misner. 1957. Comments on p. 26–27, Conference on the Role of Gravitation and Physics (mimeographed notes). Chapel Hill, North Carolina.
21. Hahn, S. G. & R. W. Lindquist. 1964. Ann. Phys. (NY) **29:** 304. Fischer, A. E. & J. E. Marsden. 1972. Comm. Math. Phys. **28:** 1.
22. Smarr, L., A. Cadež, B. DeWitt & K. Eppley. 1976. Phys. Rev. D **14:** 2443.
23. Roache, P. 1972. Computational Fluid Dynamics. Hermosa Publishers. Albuquerque, N.M.
24. Chin, R. C., J. M. Leblanc & J. R. Wilson. 1976. Lawrence Livermore Laboratory. Livermore, Calif. (private communication).
25. Emery, A. F. 1968. J. Comp. Phys. **2:** 306.
26. Matte, A. 1953. Can. J. Math. **5:** 1.
27. Zakharov, V. 1973. Gravitational Waves in Einstein's Theory. Halsted Press. Jerusalem.
28. Misner, C. W., K. S. Thorne & J. A. Wheeler. 1973. Gravitation: 466. W. H. Freeman. San Francisco.
29. Isaacson, R. A. 1968. Phys. Rev. **166:** 1272.
30. Bondi, H., M. G. J. van der Burg & A. W. K. Metzner. 1962. Proc. R. Soc. A **269:** 21.
31. Teukolsky, S. A. 1973. Astrophys. J. **185:** 644.
32. Sachs, R. K. 1962. Proc. R. Soc. A **270:** 103.
33. Zund, J. D. 1970. Tensor, N. S. **21:** 354.
34. Brill, D. R. 1959. Ann. Phys. **7:** 466.
35. Press, W. H. 1971. Astrophys. J. Lett. **170:** L105.
36. Goebel, C. J. 1972. Astrophys. J. Lett. **172:** L95.
37. Landau, L. D. & E. M. Lifshitz. 1951. The Classical Theory of Fields. Pergamon. London.
38. Zerilli, F. J. 1970. Phys. Rev. D **2:** 2141.
39. Davis, M., R. Ruffini, W. H. Press & R. H. Price. 1971. Phys. Rev. Lett. **27:** 1466.
40. Davis, M., R. Ruffini & J. Tiomno. 1972. Phys. Rev. D **5:** 2932.
41. Chung, K. P. 1973. Nuovo Cimento **14B:** 293.
42. Penrose, R. 1973. Ann. N.Y. Acad. Sci. **224:** 125.
43. Hawking, S. W. & G. F. R. Ellis. 1973. The Large Scale Structure of Spacetime. Cambridge Univ. Press. Cambridge.
44. Thorne, K. S. 1972. In Magic Without Magic: John Archibald Wheeler. J. Klauder, Ed. W. H. Freeman and Co. San Francisco.
45. Hawking, S. W. 1971. Phys. Rev. Lett. **26:** 1344.
46. Bekenstein, J. 1973. Phys. Rev. D **7:** 2333.
47. Hawking, S. W. 1976. Phys. Rev. D **13:** 191.
48. Misner, C. W. 1960. Phys. Rev. **118:** 1110.
49. Einstein, A. & N. Rosen. 1935. Phys. Rev. **48:** 73.
50. Gibbons, G. W. & B. F. Schutz. 1972. Mon. Not. R. Astron. Soc. **159:** 41P.
51. Čadež, A. 1974. Ann Phys. **83:** 449.

52. ČADEŽ, A. 1975. Ann. Phys. **91:** 58.
53. ČADEŽ, A. 1971. Ph.D. Thesis. University of North Carolina.
54. PRICE, R. H. 1972. Phys. Rev. D **5:** 2419.
55. D'EATH, P. D. 1977. High Speed Black Hole Encounters and Gravitational Radiation, Preprint (November, 1976).
56. SMARR, L. 1977. Phys. Rev. D. **15:** 2069.
57. PENROSE, R. 1976. Private communication.
58. CLARK, J. P. A. & D. M. EARDLEY. 1976. Evolution of Close Neutron Star Binaries. Preprint, Observatory and Department of Physics, Yale University (October 1976).
59. LATTIMER, J. M. & D. N. SCHRAMM. 1976. Astrophys. J. **210:** 549.
60. ZEL'DOVICH, YA. B. & I. D. NOVIKOV. 1971. Relativistic Astrophysics, Vol I. University of Chicago Press. Chicago.
61. CHRZANOWSKI, P. L. 1973. Ph.D. thesis. University of Maryland.
62. BREUER, R. A. 1975. Lecture Notes in Physics **44:** 153. Springer-Verlag. Berlin.
63. WAGONER, R. V. 1975. Astrophys. J Lett. **196:** L63.
64. SMARR, L. L. & R. BLANDFORD. 1976. Astrophys. J. **207:** 574.
65. ZEL'DOVICH, YA B. & M. A. PODURETS. 1966. Sov. Astron. AJ **9:** 742.
66. KAFKA, P. 1970. Nature **226:** 436.
67. FOWLER, W. A. 1964. Rev. Mod. Phys. **36:** 545.
68. RUFFINI, R. & J. A. WHEELER. 1971. *In* Proceedings of the Conference on Space Physics: 140. European Space Research Organization. Paris.
69. THORNE, K. S. & V. B. BRAGINSKY. 1976. Astrophys. J. Lett. **204:** L1.
70. REES, M. 1976. Paper presented at the conference on Experimental Gravitation, Pavia, Italy (September 1976).
71. TATLOR, J. H. This volume.
72. THUAN, T. X. & J. P. OSTRIKER. 1974. Astrophys. J. Lett. **191:** L105.
73. NOVIKOV, I. D. 1976. Sov. Astron. **19:** 398.
74. SHAPIRO, S. L. 1977. Astrophys. J. **214:** 566.
75. EARDLEY, D. M. 1975. Phys. Rev. D **12:** 3072.
76. KAZANAS, D. & D. N. SCHRAMM. 1976. Enrico Fermi Inst. Preprint #76: 23.
77. ARNETT, W. D. This volun.e.
78. WILSON, J. R. 1974. Phys. Rev. Lett. **32:** 849.
79. WAGONER, R. V. 1976. Preprint IIP-546, Inst. of Theoret Phys. Stanford Univ. Stanford, Calif.
80. MISNER, C. W. 1974. *In* Gravitational Radiation and Gravitational Collapse: IAU Symposium #64. C. DeWitt-Morette, Ed.: 6. D. Reidel Publishing Co. Dordrecht, the Netherlands.
81. DOUGLASS, D. H. 1976. Paper given at the International Symposium on Experimental Gravitation, Pavia, Italy (September 1976).
82. WIITA, P. J. & W. H. PRESS. 1976. Astrophys. J. **208:** 525.
83. SCHRAMM, D. N. & D. KAZANAS. Private Communication. K. O. Mikaelian 1977 Preprint FERMILAB-Pub-77132-THY.
84. RUDERMAN, M. 1972. Ann. Rev. Astron. Astrophys. **10:** 438.
85. OSTRIKER, J. P. & J. E. GUNN. 1971. Astrophys. J. Lett. **164:** L95.
86. KUNDT, W. 1976. Nature **261:** 673.
87. FRICKE, K. J. & R. KIPPENHAHN. 1972. Ann. Rev. Astron. Astrophys. **10:** 45.